Published in final edited form as:

*Curr Biol*. 2021 September 13; 31(17): 3797–3809.e5. doi:10.1016/j.cub.2021.06.048.

# Hypothalamic control of interoceptive hunger

**Justin N. Siemian**[1], **Miguel A. Arenivar**[1,2], **Sarah Sarsfield**[1], **Yeka Aponte**[1,3]

[1]Neuronal Circuits and Behavior Unit, National Institute on Drug Abuse Intramural Research Program, National Institutes of Health, Baltimore, MD 21224-6823, U.S.A.

[2]Current Affiliation: Brown-NIH Graduate Partnership Program, Brown University, Providence, RI 02912, U.S.A.

[3]The Solomon H. Snyder Department of Neuroscience, Johns Hopkins University School of Medicine, Baltimore, MD 21205, U.S.A.

## Summary

While energy balance is critical to survival, many factors influence food intake beyond caloric need or "hunger." Despite this, some neurons that drive feeding in mice are routinely referred to as "hunger neurons," whereas others are not. To understand how specific hypothalamic circuits control interoceptive hunger, we trained mice to discriminate fasted from sated periods. We then manipulated three hypothalamic neuronal populations with well-known effects on feeding while mice performed this task. While activation of $ARC^{AGRP}$ neurons in sated mice caused mice to report being food-restricted, $LH^{VGAT}$ neuron activation or $LH^{VGLUT2}$ neuron inhibition did not. In contrast, $LH^{VGAT}$ neuron inhibition or $LH^{VGLUT2}$ neuron activation in fasted mice attenuated natural hunger, whereas $ARC^{AGRP}$ neuron inhibition did not. Each neuronal population evoked distinct effects on food consumption and reward. After satiety- or sickness-induced devaluation, $ARC^{AGRP}$ neurons drove calorie-specific feeding, while $LH^{VGAT}$ neurons drove calorie-indiscriminate food intake. Our data support a role for $ARC^{AGRP}$ neurons in homeostatic feeding and implicate them in driving a hunger-like internal state that directs behavior toward caloric food sources. Moreover, manipulations of LH circuits did not evoke hunger-like effects in sated mice, suggesting that they may govern feeding more related to reward, compulsion, or generalized consumption than to energy balance but also that these LH circuits can be powerful

Lead Contact: Yeka Aponte (yeka.aponte@nih.gov).

Author contributions

Conceptualization, J.N.S. and Y.A.; Methodology, J.N.S. and Y.A.; Validation, J.N.S. and Y.A.; Formal analysis, J.N.S. and Y.A.; Investigation, J.N.S., M.A.A., and S.S.; Resources, S.S. and Y.A.; Data curation, J.N.S.; Writing – original draft, J.N.S., S.S., and Y.A.; Writing – review and editing, J.N.S., M.A.A, S.S., and Y.A.; Visualization, J.N.S., S.S., and Y.A.; Supervision, Y.A.; Project administration, Y.A.; Funding acquisition, Y.A.



Inclusion and diversity

One or more of the authors of this paper self-identifies as an underrepresented ethnic minority in science. One or more of the authors of this paper received support from a program designed to increase minority representation in science. The author list of this paper includes contributors from the location where the research was conducted who participated in the data collection, design, analysis, and/or interpretation of the work.

Declaration of interests

The authors declare no competing interests.

negative appetite modulators in fasted mice. This study highlights the complexity of hypothalamic feeding regulation and can be used as a framework to characterize how other neuronal circuits affect hunger and identify potential therapeutic targets for eating disorders.

## eTOC

Using a behavioral paradigm for mice to discriminate feelings of “hunger” from satiety, Siemian et al. investigate the contributions of hypothalamic neuronal subtypes to interoceptive hunger. They show that arcuate nucleus AGRP neurons drive a hunger-like internal state, whereas GABAergic and glutamatergic lateral hypothalamic neurons do not.

## Introduction

Regulating food intake is essential for survival. Food-oriented behavior in basic research is typically presented in terms of *homeostatic feeding*—food intake necessary to maintain normal body weight—or *hedonic feeding*—food intake motivated by gustatory sensation or reward[1,2]. These distinctions are clearly applicable to humans, who eat to satisfy homeostatic energy demands but also for pleasure, such as ingesting desserts high in fat and sugar even after a large meal. Thus, understanding the neuronal circuits controlling homeostatic and hedonic feeding may help to address diseases associated with overeating and undereating such as obesity and anorexia nervosa, respectively.

Many neuronal circuits can simultaneously influence food intake and reward, suggesting extensive overlap between homeostatic and hedonic feeding systems[1]. For example, activation of γ-aminobutyric acid (GABA)-expressing neurons in the lateral hypothalamus (LH; $LH^{VGAT}$ neurons) evokes food intake and is rewarding[3], whereas activation of LH glutamatergic ($LH^{VGLUT2}$) neurons decreases food intake and is aversive[4]. Further downstream, the activation of ventral tegmental area (VTA) GABAergic neurons inhibits reward consumption and drives aversion[5,6], while VTA dopaminergic neurons promote food seeking and reward[7]. Yet among these and other cell populations that modulate feeding, only arcuate hypothalamic agouti-related peptide-expressing ($ARC^{AGRP}$) neurons are routinely referred to as homeostatic feeding-related “hunger” neurons[8–16]. This anthropomorphic terminology may have resulted from some interesting properties that $ARC^{AGRP}$ neurons possess. For example, their activity increases during periods of caloric deficit and decreases in a calorie-dependent manner following the detection and ingestion of a food source[10,14,17–19]. Moreover, activation of $ARC^{AGRP}$ neurons recapitulates many of the behavioral and neuronal changes induced by food restriction[9,11,15,20–25]. However, even the activity of these “homeostatic” feeding neurons has not been dissociated from overlapping reward processes. One study found that $ARC^{AGRP}$ neuronal activation imparts a negative valence, since mice become averse to flavors and places repeatedly paired with it[10]. This finding predicted that the inhibition of $ARC^{AGRP}$ neurons by food detection and consumption transmits a teaching signal via negative reinforcement (the removal of the negative stimulus). However, the inability of food-restricted mice to acquire simple operant tasks to cease $ARC^{AGRP}$ neuronal stimulation does not support negative reinforcement as the primary driver of their effects on food intake[8,10]. Alternatively, another study suggested that $ARC^{AGRP}$ neurons drive feeding through a long-lasting positive valence signal, as mice

develop a preference for flavors and foods accessible following pre-stimulation of $ARC^{AGRP}$ neurons (and not concurrent stimulation)[8]. Moreover, mice self-administered short bursts of optogenetic activation of $ARC^{AGRP}$ neurons when food was also accessible[8]. $ARC^{AGRP}$ neuronal activation was also recently shown to potentiate a dopamine response to food, further depicting the overlap between circuits for homeostasis and reward[26]. Thus, while these studies together may form a unified model to account for the contribution of $ARC^{AGRP}$ neuronal activity to food-oriented behavior, their findings do more to characterize how $ARC^{AGRP}$ neurons influence reward rather than hunger.

"Hunger" is a subjective experience, and in rodents is an inferred motivational state generally defined according to the operation that produces it—food deprivation—or the effect it produces—food intake[27]. While humans can easily answer whether they are "hungry" or "sated," the same does not apply to rodents. Mice and rats eat for reasons other than food deprivation[28–30] and feeding does not always follow food deprivation[31–35]. Therefore, measures of food intake do not distinguish hunger from the multiple factors that affect feeding and, by extension, $ARC^{AGRP}$ neuronal activity may not truly encode for hunger. Furthermore, as described nearly 50 years ago, hypothalamic stimulation-induced behavior tends to be unusually rigid[27]. For instance, rats do not switch to consume a different food when an LH stimulation-paired food is removed[36], and $LH^{VGAT}$ neuron activation in mice can evoke consummatory behavior even when food is not available[3]. Similar findings have been reported for $ARC^{AGRP}$ neuron stimulation, which drives stereotypic behaviors beyond feeding in the absence of food such as locomotion, digging, grooming, and marble burying[37]. Therefore, to distinguish homeostatic from hedonic feeding-related circuits, and whether these circuits mediate hunger-like states, calls for investigations of behavior extending beyond simple food intake have been raised[1].

Drug discrimination experiments have been used for decades to understand the interoceptive effects of pharmacological compounds and to gain a more detailed understanding of their actions that extend beyond their simple reinforcing effects[38,39]. For example, both cocaine and heroin are readily self-administered[40–43], but they do not produce a common discriminative stimulus[44,45]. That is, each drug triggers a reinforcing, yet distinct, interoceptive experience. A similar scenario may exist among neuronal populations that drive feeding, where some evoke a sensation of hunger and others do not. However, only a small number of studies have used discrimination techniques to examine differences in the interoceptive features produced by food satiety or food restriction[46–48]. In these studies, some pharmacological manipulations that alter food intake in rats also change the interoceptive cue associated with food restriction or satiety, whereas others do not, suggesting divergent feeding-associated drives[49–52]. However, such methods have not been used to understand the subjective effects associated with cell type- or circuit-specific manipulations that evoke or suppress feeding. Here we apply an operant "hunger discrimination" paradigm in combination with optogenetics and chemogenetics to determine the roles of $ARC^{AGRP}$, $LH^{VGAT}$, and $LH^{VGLUT2}$ neurons in regulating interoceptive hunger cues in mice. In addition, we directly compare the feeding- and reward-associated effects of these neuronal populations and assess whether they drive calorie-specific or indiscriminate feeding.

## Results

### Hypothalamic control of hunger- and satiety-associated interoceptive cues

We first determined whether mice could discriminate periods of food restriction (22-h food deprivation, 'fasted') from periods of food satiety (1-h food deprivation, 'sated'). On fasted training days, food was removed from the home cage 22 h before the operant session. Responses on one designated active lever (e.g., left) were reinforced with sucrose pellets (fixed ratio 15, 5 pellets maximum), whereas responses on the opposite lever reset the response requirement on the active lever. On sated training days, food was removed from the home cage 1 h before the operant session, and the lever contingencies were reversed. Responses on the opposite lever (e.g., right) were then reinforced with sucrose pellets, whereas responses on the other lever reset the requirement on the now-active lever (Figure 1A). Sated and fasted sessions were administered according to a generally double alternating schedule (i.e., sated, sated, fasted, fasted)[53]. Within the first 50 sessions, average responding of all mice approached the 80% threshold for feeding status-appropriate responding (Figure 1B). Individual mice qualified for testing by performing greater than 80% appropriate responding in 5 consecutive or 6 out of 7 consecutive sessions[47,49–57] (Figure 1C). The mean number of sessions until meeting these qualification criteria was 60 (median: 50, range: 17 – 182, Figure 1D). Mice were then given two free-choice test sessions, one in the sated condition and one in the fasted condition, during which sucrose pellets could be earned by responses at either lever to verify stimulus control (Figures 1A and E; top panel) and engagement in the task during both sessions (Figure 1E; bottom panel). Following these tests, mice were randomly assigned within each genotype to receive Cre recombinase-dependent experimental (ChR2-YFP + hM4D-mCherry) or control (YFP + mCherry) viral cocktail injections in the ARC of *Agrp*$^{Cre}$ mice[58,59] or in the LH of *Vgat*$^{Cre}$ and *Vglut2*$^{Cre}$ mice[60] with optical fibers implanted above the ARC or LH, respectively (Figures 2A–C). Using this previously validated dual-virus approach[61], we next examined the effects of activating and inhibiting these specific hypothalamic populations on interoceptive hunger.

Following surgical recovery and brief retraining, mice were exposed to free-choice test sessions while we manipulated neuronal activity with optogenetics or chemogenetics to assess the potential bidirectional effects of these three specific hypothalamic cell types on the perceived feeding status. Photostimulation of sated ARC$^{AGRP}$:ChR2/hM4D mice significantly increased fasted-associated lever responding in a frequency-dependent manner (Figure 2D; top panel). At the highest frequency tested (i.e., 20 Hz), and the one most commonly used in ARC$^{AGRP}$ studies[8,10,15,23], mice exceeded the 80% fasted-appropriate responding threshold, indicating the induction of an interoceptive discriminative stimulus similar to the 22-h fasted condition. However, chemogenetic inhibition of ARC$^{AGRP}$ neurons in fasted ARC$^{AGRP}$:ChR2/hM4D mice via 1 h CNO pretreatment (1 mg/kg, i.p.) did not significantly decrease fasted-associated lever responding (Figure 2E; top panel). In a separate test, 4 h CNO pretreatment also did not significantly decrease fasted-associated lever responding (83.11 ± 7.78%). Neither ARC$^{AGRP}$ neuronal activation nor inhibition affected the response rate (Figures 2D–E; bottom panels), suggesting that the changes in lever responding during manipulations of ARC$^{AGRP}$ neurons were not triggered by changes in motor coordination or motivation to obtain the sucrose pellets. Furthermore, no

changes in lever choice or response rate were observed during photostimulation or clozapine *N*-oxide (CNO) injection in $ARC^{AGRP}$:YFP/mCherry control mice (Figures 2D–E; top and bottom panels), demonstrating no off-target effects of these manipulations[62–64]. Thus, while $ARC^{AGRP}$ neurons appear sufficient to evoke a hunger-like interoceptive state in sated mice, they are not necessary for maintaining this state in fasted mice.

Contrasting results were observed during manipulations of lateral hypothalamic neurons. Photostimulation of sated $LH^{VGAT}$:ChR2/hM4D mice did not significantly increase fasted-associated lever responding, and these mice did not approach 80% fasted-lever responding at any of the photostimulation frequencies tested (Figure 2F; top panel). However, chemogenetic inhibition of $LH^{VGAT}$ neurons in fasted $LH^{VGAT}$:ChR2/hM4D mice did significantly decrease fasted-associated lever responding (Figure 2G; top panel). Neither manipulation affected the response rate in these sessions, and no changes in lever responding or response rate in $LH^{VGAT}$:YFP/mCherry control mice were observed (Figures 2F–G; top and bottom panels). These results suggest that $LH^{VGAT}$ neurons are not sufficient to evoke hunger in sated mice but are necessary for maintaining a hunger-like interoceptive state in fasted mice.

We last examined the effects of $LH^{VGLUT2}$ neuronal manipulations in this task. Since $LH^{VGLUT2}$ neuron activation has previously been shown to decrease food intake[4,9], we photostimulated fasted $LH^{VGLUT2}$:ChR2/hM4D mice during testing. Strikingly, we observed that all of the photostimulation frequencies tested significantly decreased fasted-associated lever responding (Figure 2H; top panel). However, higher frequencies also decreased the response rate (Figure 2H; bottom panel), suggesting effects on motivation or motor coordination, or the induction of other aversive-like effects[4]. However, no effects of chemogenetic inhibition of these neurons in sated $LH^{VGLUT2}$:ChR2/hM4D mice were observed (Figure 2I; top panel), and neither manipulation affected the behavior of $LH^{VGLUT2}$:YFP/mCherry control mice (Figures 2H–I; top and bottom panels). Thus, $LH^{VGLUT2}$ neurons appear to be potent appetite suppressors, but at higher stimulation frequencies, they also seem to disrupt normal operant behavior. Together, these results indicate that the activity of $LH^{VGLUT2}$ neurons is sufficient but not necessary for satiety-like interoceptive states.

To further characterize this operant model in mice, we also tested several pharmacological compounds previously shown to alter food intake in rodents[58,65–70] and/or cause weight loss in humans[71,72]. Similar to the findings of previous studies in rats[49–52], some of these compounds (the orexigenic hormone ghrelin and the anorexigenics liraglutide or combination of naltrexone/bupropion) significantly changed feeding status-appropriate responding, whereas others (the anorexigenics rimonabant, lorcaserin, and or phentermine) did not (Figure S1). Together, these results show that out of many neuronal or pharmacological manipulations previously shown to alter food intake, only some appear to affect interoceptive hunger. Thus, simple measurements of food intake are likely an unreliable indicator of interoceptive hunger.

### Hypothalamic control of food intake and reward-related behavior

We next directly compared the effects of these three hypothalamic populations on feeding and reward-related behaviors. In a context distinct from the previous operant experiments, we first measured the free-access intake of food pellets that have identical composition to standard chow but novel shape and texture (Figure 3A). The novelty of the test chamber and food, combined with testing during the light cycle, was by design to make baseline food intake very low. We found that $ARC^{AGRP}$ neuronal activation in sated mice triggered significant intake of the novel food pellets in the novel context (Figure 3B), and that this effect became more robust during a second photostimulation test (Figure 3C) following three days of habituation to the food pellets and context without photostimulation. Chemogenetic inhibition of $ARC^{AGRP}$ neurons in food-restricted mice decreased intake of home cage standard chow by 4 h post-food access (Figure 3D), indicating that inhibition of these neurons may cause an effect more similar to early satiety than a general suppression of feeding. CNO did not affect feeding in control mice (Figure 3D), suggesting that no off-target effects occurred[63]. In the real-time place preference assay, activation of $ARC^{AGRP}$ neurons did not evoke significant rewarding or aversive effects (Figures 3E–F and S2A). Thus, $ARC^{AGRP}$ neuronal activity bidirectionally modulates food intake but does not appear to affect reward-related behaviors in the absence of food.

By contrast, $LH^{VGAT}$ neuronal activation did not evoke consumption of the novel food pellets (Figure 3G), only triggering intake following habituation (Figure 3H). Moreover, inhibition of $LH^{VGAT}$ neurons in food-restricted mice decreased home cage standard chow intake across the entire testing period (Figure 3I), indicating a more generalized suppressive effect on feeding as compared to $ARC^{AGRP}$ neuronal inhibition. Furthermore, photostimulation of $LH^{VGAT}$ neurons also triggered significant rewarding effects in the real-time place preference assay (Figures 3J–K and S2B), consistent with previous studies showing the robust effects on reward-like behavior mediated by these neurons[3].

Activation of $LH^{VGLUT2}$ neurons in food-restricted mice significantly decreased standard chow intake (Figures 3L–M) in agreement with previous findings[4]. Chemogenetic inhibition of $LH^{VGLUT2}$ neurons in sated mice did not alter standard chow intake in sated or food-restricted mice (Figures 3N and S3A) nor did it affect the intake of several other caloric and palatable food sources tested (Figures S3B–D), in contrast to previous studies that reported slight yet significant increases in food intake during $LH^{VGLUT2}$ inhibition[4,9]. We speculated that $LH^{VGLUT2}$ neuronal inhibition may drive the consumption of food that mice would normally not eat in large amounts. With access to a palatable non-caloric gel, $LH^{VGLUT2}$ inhibition increased gel intake, whereas control mice ate very little (Figure 3O), perhaps reflecting the negative feedback normally occurring during ingestion of such a calorie-free food source. Moreover, we observed that photostimulation of $LH^{VGLUT2}$ neurons triggered significant real-time place avoidance (Figures 3P–Q and S2C), consistent with previous reports[4].

To characterize any potential overt behavioral changes, locomotor impairments, or alterations in anxiety-like behavior triggered by the functional inhibition of these hypothalamic populations, we tested sated mice in the open field paradigm. Chemogenetic inhibition of $ARC^{AGRP}$ neurons increased time spent in the center of the apparatus but

did not affect total distance or maximum speed (Figures S4A–D), indicating anxiolytic-like effects consistent with previous findings[22]. $LH^{VGAT}$ neuronal inhibition decreased both total distance and maximum speed (Figures S4E–H), whereas inhibition of $LH^{VGLUT2}$ neurons increased total distance (Figures S4I–L). These results support the opposing behavioral roles of these LH populations[3,4] and suggest that locomotor activity, in addition to food intake and reward, is under opposing regulation by $LH^{VGAT}$ and $LH^{VGLUT2}$ circuits.

## Hypothalamic feeding circuits are distinguished by calorie-specific versus indiscriminate food intake

Since activation of both $ARC^{AGRP}$ and $LH^{VGAT}$ neurons triggers food intake[3,8,10,15,25], and we have demonstrated here that only $ARC^{AGRP}$ activation evokes a hunger-like interoceptive cue, we last compared the effects of activating these two specific hypothalamic cell types on caloric and non-caloric food intake under states of satiety- or sickness-induced devaluation. We predicted that the hunger-like, homeostatic drive evoked by $ARC^{AGRP}$ activation would direct behavior specifically toward caloric food under conditions of devaluation, whereas the motivational drive evoked by $LH^{VGAT}$ neuronal activation would drive indiscriminate food intake regardless of caloric content. It was previously shown that $ARC^{AGRP}$ neuronal responses are rapidly trained by the caloric content of gel[18], thus we used two gels of different flavor and caloric content (one sweetened with sucrose and one sweetened with sucralose). Mice should rapidly learn and prefer the calorie-containing gel but also find the artificially-sweetened non-caloric gel palatable[73], as opposed to non-palatable control targets such as plastic or cellulose pellets which are rarely consumed[4,74]. For satiety-induced devaluation (Figure 4A), mice had simultaneous access to both caloric (strawberry flavor) and non-caloric (orange flavor) gel for 30-min test sessions. While *ad libitum*-fed mice normally displayed preference for the caloric gel over the non-caloric gel (Figures 4B–C, ‘Not prefed’), 1-h pre-exposure to the caloric gel significantly decreased caloric gel intake during the test session but did not increase non-caloric gel intake (Figures 4B–C, ‘CG prefed’). Strikingly, $ARC^{AGRP}$ neuronal activation following 1-h caloric gel pre-exposure selectively restored caloric gel intake during the test session (Figures 4B, ‘CG prefed + stim’), whereas activation of $LH^{VGAT}$ neurons triggered increases in both caloric and non-caloric gel intake (Figure 4C, ‘CG prefed + stim’). Thus, $ARC^{AGRP}$ neuronal activity appears to guide specific intake of caloric food even under conditions of sensory and caloric satiety, whereas $LH^{VGAT}$ activity drives indiscriminate food intake unrelated to caloric content.

To further elucidate the effects of manipulating these neuronal populations on devalued food intake, we used sickness-induced devaluation with lithium chloride (LiCl; Figure 4D). When administered after animals consume a novel food, LiCl induces gastrointestinal malaise and decreases subsequent intake of that food by learned negative associations (i.e., conditioned taste aversion)[75–77], as opposed to the active physiological satiety cues in the previous test (Figures 4A–C). For this, mice were exposed to a novel caloric gel for 1 h (peach flavor) and then immediately given an intraperitoneal (i.p.) injection of LiCl (6 mEq/kg) to induce gastrointestinal malaise and taste aversion. The following day, mice were again exposed to the caloric gel during photostimulation, and activation of either $ARC^{AGRP}$ or $LH^{VGAT}$ neurons significantly restored intake of the caloric gel relative to their respective

control mice (Figures 4E and G). This procedure was repeated 3 days later using a novel non-caloric gel (cherry flavor). While no changes from control mice were observed during $ARC^{AGRP}$ neuronal activation, photostimulation of $LH^{VGAT}$ neurons significantly increased non-caloric gel intake following LiCl devaluation (Figures 4F and H). Together, these results demonstrate that both $ARC^{AGRP}$ and $LH^{VGAT}$ neurons can drive food intake despite conditions of devaluation. Our findings support a role for $ARC^{AGRP}$ neurons in driving calorie-specific food intake. Here, we demonstrate for the first time that $ARC^{AGRP}$ neurons encode a discriminable hunger-like interoceptive state to mediate homeostatic feeding. In contrast, the calorie-independent food intake observed during activation of $LH^{VGAT}$ neurons suggests that these neurons likely mediate generalized consummatory or compulsive-like feeding.

## Discussion

Understanding whether behavior reflects the internal state of an animal is a fundamental challenge of neuroscience. We, as humans, realize that many behaviors rely on internal feelings, such as reflexive withdrawal from pain or eating when hungry. However, these behaviors are not always exclusive to the preceding internal state. One may withdraw a hand due to surprise as opposed to pain or eat despite a lack of hunger. Then again, the lack of a behavioral response does not necessarily indicate the absence of a particular internal state. For instance, a boxer may not eat despite extreme hunger when trying to make a weight class or persist in a match despite being injured and in physical pain. As cutting-edge techniques continue to identify specific circuits involved in behavioral control, understanding the effects of these manipulations on the internal sensations of the subject will be required to draw accurate conclusions regarding behavior.

To this end, we assessed three hypothalamic neuronal populations with well-characterized effects on food intake for their ability to modulate interoceptive hunger- and satiety-like states. Between $ARC^{AGRP}$ and $LH^{VGAT}$ neurons that trigger feeding when activated, only $ARC^{AGRP}$ neurons evoked significant increases in hunger-like responding. This finding, coupled with $ARC^{AGRP}$ neurons driving calorie-specific food intake, strongly supports a role for $ARC^{AGRP}$ neurons in mediating homeostatic feeding and hunger. Importantly, the lack of aversive effects of $ARC^{AGRP}$ neuronal activation during the RTPP test in our study are not at odds with previous reports, which only observed aversive effects after several pairing sessions[10]. In contrast, activation of $LH^{VGAT}$ neurons increased intake of familiar but not novel food, induced rewarding effects, and triggered calorie-indiscriminate feeding, suggesting these neurons are more involved in generalized consummatory behavior rather than homeostatic feeding. Notably, $LH^{VGAT}$ neuronal activation did not interfere with the responding rate in this task, suggesting that the lack of hunger-like responding did not result from a generalized disruption of operant performance. Interestingly however, $LH^{VGAT}$ but not $ARC^{AGRP}$ inhibition decreased hunger-like responding, which accords with the more robust decrease in food intake by $LH^{VGAT}$ inhibition. This decrease was also importantly not due to a disruption of operant behavior, as the lever pressing rate was unaffected by $LH^{VGAT}$ inhibition. The inability of $ARC^{AGRP}$ inhibition to suppress physiological hunger in the operant paradigm is not altogether surprising, as our study and those of others show that $ARC^{AGRP}$ neurons are generally less amenable to inhibition than activation via optogenetic

or chemogenetic methods[8,22,25]. The explanation for this phenomenon is currently unclear. Since the activity of only 800 $ARC^{AGRP}$ neurons is sufficient to induce feeding[15], it is possible that our chemogenetic viral strategy did not inhibit enough $ARC^{AGRP}$ neurons to attenuate feeding. However, this is not likely due to the co-administration of AAVs, which has been demonstrated in many studies to remain a viable viral strategy without between-virus interference[78–80]. Instead, the gradual suppression of feeding observed during $ARC^{AGRP}$ neuronal inhibition in the food intake experiment functionally validates the strategy indicating that there was sufficient chemogenetic inhibition of these neurons and accords with previous reports that the suppression of feeding by $ARC^{AGRP}$ neuronal inhibition is related to premature cessation of feeding rather than a generalized decrease in feeding[9,25,81–83]. Of note, our chemogenetic inhibition of $ARC^{AGRP}$ neurons in this study caused the exact same pattern of suppressed feeding as previously observed[25]. As such, current evidence suggests that the more subtle behavioral effects of $ARC^{AGRP}$ inhibition are not related to technical issues but are simply a byproduct of the primarily unidirectional appetitive effects of $ARC^{AGRP}$ circuitry on food intake.

To tie these results to the prevailing mechanistic understanding of $ARC^{AGRP}$ neuronal activity, previous studies suggest that during physiological hunger, $ARC^{AGRP}$ neurons are highly active and release neurotransmitters such as GABA, AGRP, and neuropeptide Y (NPY) to downstream brain regions such as the paraventricular hypothalamus (PVH)[84]. Once this happens, food seeking and intake occur even in the absence of concurrent $ARC^{AGRP}$ neuronal activity[8,84], suggesting that these effects are long-lasting and dependent on brain regions and neuronal circuits outside the ARC. When a mouse detects and/or consumes a food source, $ARC^{AGRP}$ neuronal activity drops proportionately to the perceived and actual energy content of the food, such that more caloric foods induce larger and longer-lasting inhibition of AGRP neuronal activity[16–18,85]. This activity then gradually recovers prior to triggering a subsequent feeding bout, and this cycle continues until enough calories have been consumed to meet current homeostatic need. In this light, chemogenetic inhibition of $ARC^{AGRP}$ neurons is likely either (a) not powerful enough to suppress ongoing $ARC^{AGRP}$ activity caused by 22-h food restriction or (b) incapable of reversing the effects triggered in downstream brain regions like the PVH to reduce initial feeding bouts. Instead, $ARC^{AGRP}$ inhibition seems capable of potentiating the natural decrease in neuronal activity following food intake and/or attenuating the recovery of neuronal activity to decrease feeding in later bouts. In other words, $ARC^{AGRP}$ inhibition does not affect the rate of feeding early in a meal but may cause an individual to “feel full” earlier within a meal or longer after a meal, akin to bariatric surgery in humans, effectively limiting overall food consumption within and/or across meals. In our study, since mice were food-restricted for 22 h prior to the “fasted” tests in the hunger discrimination task, $ARC^{AGRP}$ neuron inhibition did not alter natural hunger cues. However, it is likely that $ARC^{AGRP}$ inhibition would decrease the amount of food required for a mouse to report feeling sated in this task. Interestingly, the more robust effects of $LH^{VGAT}$ inhibition on feeding and hunger-like responding in food restricted mice support previous predictions that both homeostatic and hedonic circuits are active during all feeding conditions, albeit likely to different degrees depending on the food source and physiological conditions[1]. In this context, during acute manipulations, circuits in

the LH may be necessary but not sufficient for hunger, whereas circuits in the ARC may be sufficient but not necessary for hunger.

One point warranting further discussion is the effect of hypothalamic activation on calorie preference during the gel intake tests in the current study. Previous work showed that taste-blind mice can develop preference for caloric sweeteners but not for non-caloric sweeteners, and that sucrose intake uniquely induced dopamine release in the ventral striatum, suggesting that calories can directly influence reward circuitry independent of taste[86]. Since $ARC^{AGRP}$ activation does not generally evoke dopamine release but instead potentiates dopamine responses selectively to food, this likely explains why mice maintained specific preference for the caloric gel. In contrast, the generalized increase on dopamine release by $LH^{VGAT}$ activation[87] likely explains why mice did not discriminate between gels, as dopamine signaling was artificially increased enough to drive intake of the non-caloric gels and lower caloric discrimination. Relatedly, learning a behavioral task is also heavily dopamine-dependent, and the effects of $ARC^{AGRP}$ activity on learning have been a subject of intense interest in previous studies[8,10]. However, these studies mainly examined the role of $ARC^{AGRP}$ activity on learning the caloric value of a food rather than learning the consequences of an action. Since we carefully controlled the amount of training in each physiological condition in the hunger discrimination task, we do not think that hypothalamic activation in the current study influenced the expression of a differentially learned behavior to obscure test results. Instead, behavior must have been guided by the elicited interoceptive information from the specific neuronal type being manipulated.

Our findings also further elucidate a role for $LH^{VGLUT2}$ neurons as a powerful brake on food intake. Known to trigger aversion and decreases in feeding[4], $LH^{VGLUT2}$ neurons were more recently shown to encode satiety state and undergo modulation following chronic intake of a high fat diet[88]. Together, these pieces support a role for $LH^{VGLUT2}$ neuronal activity in the promotion of satiety cues. However, higher activation frequencies of $LH^{VGLUT2}$ neurons caused a decrease in the ability of the mice to perform the hunger discrimination task, likely due to aversive-like effects. Although $LH^{VGLUT2}$ activation at low frequencies may also induce aversive effects[4] that secondarily suppress hunger, our results at least reveal overlap between motivational and homeostatic mechanisms. Though we did not find evidence that acute chemogenetic $LH^{VGLUT2}$ inhibition increased intake of caloric food sources, contrary to the small effects previously reported[9], imaging and ablation studies suggest that changes in $LH^{VGLUT2}$ neuron activity generally precede behavioral consequences[88,89], and thus more chronic inhibition of these neurons may be required to observe changes in food intake. Moreover, $LH^{VGLUT2}$ neuron inhibition did increase non-caloric gel intake. Since control mice consumed very little of the gel as it was novel and non-nutritive, the increase during $LH^{VGLUT2}$ inhibition supports a role for these neurons in normally inhibiting inappropriate food intake (e.g., if a food is devoid of nutrients). In concept, this role could be readily translated to pathological conditions like overeating when normal satiety feedback signals are insufficient to cease feeding beyond appropriate amounts[88]. Nevertheless, the changes in open field behavior by $LH^{VGLUT2}$ neuron inhibition, which were opposite to those during $LH^{VGAT}$ inhibition, also corroborate the acute functional inhibition of these neurons.

Future work will be needed to further unravel interactions between $ARC^{AGRP}$ neurons and circuits within the LH. It is currently known that $ARC^{AGRP}$ neurons directly innervate both $LH^{VGAT}$ and $LH^{VGLUT2}$ neurons[9], but how the activity of these circuits might be differentially affected remains less clear. Brain slice electrophysiological recordings using ChR2-assisted circuit mapping (CRACM) have only been performed between $ARC^{AGRP}$ and LH orexin-expressing neurons, which were shown to be inhibitory synapses[90]. LH orexin neurons are mainly glutamatergic, but some may be GABAergic[91]. Moreover, activation of $ARC^{AGRP}$ neurons was shown to inhibit and induce long-term depression in postsynaptic neurons of several other projection regions[92]; while the LH was not studied, it is likely that the same phenomenon occurs in both $LH^{VGAT}$ and $LH^{VGLUT2}$ neurons. Deciphering the significance of this on feeding drives will likely prove an interesting line of future research.

Relatedly, the higher order brain regions responsible for the conscious perception of interoceptive hunger driven by these hypothalamic neuronal populations remain largely unstudied. Although $ARC^{AGRP}$ neurons only send direct axonal projections to subcortical brain regions[93], chemogenetic activation of $ARC^{AGRP}$ neurons evoked increased activity in several higher brain areas, including the hippocampus and multiple cortical regions[94]. Yet, the only detailed characterization of $ARC^{AGRP}$ activity on individual cortical neurons has been performed in the insular cortex, a critical site for interoception[95,96]. $ARC^{AGRP}$ activation in sated mice caused insular cortical neurons to respond to visual cues similarly to physiological food restriction[20,21]. The pathway from $ARC^{AGRP}$ neurons to the insular cortex was trisynaptic, passing through the paraventricular nucleus of the hypothalamus and the basolateral amygdala, indicating that several layers and types of information are likely integrated in this system. Characterizing how $ARC^{AGRP}$ neurons and LH neuronal subpopulations affect cortical processing as it pertains to interoception will likely be a fruitful line of future research. Furthermore, conducting similar “hunger discrimination” paradigms using alternative reinforcement strategies such as shock avoidance, which removes the potential motivational confound of food in the current and previous studies, will be an important component to reveal the effects of these and other neuronal populations on interoceptive drives.

In summary, this is the first study to use an operant discrimination task to determine how specific neuronal circuits modulate interoceptive hunger and satiety states. While we confirm previous theories that $ARC^{AGRP}$ neurons evoke hunger and homeostatic feeding, we also find complex roles for feeding circuits in the LH that can influence interoceptive hunger cues in food-restricted mice. Therefore, our study provides a versatile framework for future circuit-specific investigations of the interoceptive sensations of hunger or other complex motivational states.

## STAR methods

### Resource availability

**Lead contact—**Further information and requests for resources and reagents should be directed to and will be fulfilled by Yeka Aponte (yeka.aponte@nih.gov).

**Materials availability—**This study did not generate new unique reagents.

## Data and code availability

- All data reported in this paper will be shared by the lead contact upon request.
- This paper does not report original code.
- Any additional information required to reanalyze the data reported in this paper is available from the lead contact upon request.

## Experimental model and subject details

**Animals—**All experimental protocols were conducted in accordance with U.S. National Institutes of Health Guidelines for the Care and Use of Laboratory Animals and with the approval of the National Institute on Drug Abuse Animal Care and Use Committee. Heterozygous *Agrp*$^{Cre}$ (*Agrp*$^{tm1(cre)Lowl}$; C57BL/6J background; Strain 12899, The Jackson Laboratory, ME, USA), *Vgat*$^{Cre}$ (*Slc32a1*$^{tm2(cre)Lowl}$; C57BL/6J background; Strain 28862, The Jackson Laboratory), and *Vglut2*$^{Cre}$ (*Slc17a6*$^{tm2(cre)Lowl}$; C57BL/6J background; Strain 28863, The Jackson Laboratory) male and female mice were used in this study. Mice were maintained at the National Institute on Drug Abuse Intramural Research Program animal facility under standard housing conditions. From the onset of operant training, mice were individually housed under a 12-hour light-dark cycle at 20 – 24 °C and 40 – 60% humidity with free access to water and food (“chow”; PicoLab Rodent Diet 20, 5053 tablet, LabDiet/Land O’Lakes Inc., MO, USA) unless otherwise stated.

**Hunger discrimination training procedure—**Daily discrimination sessions were conducted in six standard two-lever operant conditioning chambers (Coulbourn Instruments, LLC, PA, USA) housed inside sound-attenuating, ventilated cubicles. 20-mg sucrose pellets (PicoLab Rodent Test Diet sucrose rewards 5TUT) reinforced lever pressing and were delivered by a pellet dispenser into an extended pellet delivery trough (Coulbourn) located between the two retractable response levers. A house light located in the back panel of the operant chamber was illuminated during active response periods during experimental sessions. Experimental contingencies and data collection were executed via Graphic State v4 software (Coulbourn).

To begin operant training, mice were food-restricted to approximately 90% of their free-feeding bodyweight (fed 2.5 to 3.0 g chow per day) and trained to lever press for sucrose pellets. Mice were weighed prior to sessions performed five to seven days per week (one session daily). Initially, a single lever press was reinforced with a 20-mg sucrose pellet, and response requirements were gradually increased according to individual performance until 15 lever presses (fixed ratio 15; FR15) were required to produce sucrose pellets[49–51]. When responding reliably occurred at both levers, mice were given free access to food for 3 days before discrimination training began. Mice were then trained to discriminate between periods of fasting and satiety. Under ‘fasted’ conditions, food was removed 22 h before the training session. Mice were placed into the operant chambers for a 10-min habituation period after which the house light was illuminated, both levers were extended into the chamber, and 15 lever presses at one designated active lever (e.g., left) were reinforced with a 20-mg sucrose pellet under the FR15 reinforcement schedule. Incorrect (e.g., right) lever presses reset the response requirement on the active lever[53] but had no programmed

consequence otherwise. The session continued until five reinforcers were earned or 20 min elapsed. Under ‘sated’ conditions, food was removed 1 h before the training session and contingencies were reversed. The previously ‘incorrect’ lever (e.g., right) was now reinforced with sucrose pellets under the FR15 schedule, and the responses at the other lever (e.g., left) now reset the response requirement at the ‘sated’ lever. Conditions were administered according to a roughly double-alternating schedule (i.e., fasted, fasted, sated, sated) according to individual performance. Discrimination training continued for each mouse until they emitted at least 80% condition-appropriate responding over the entire session for either five consecutive daily sessions or six out of seven consecutive sessions.

We used the incorrect lever to reset the correct lever responses to discourage ‘trial-and-error’ strategies. Our pilot experiments followed previously used rat protocols that punished 15 incorrect lever responses with an 8-s timeout period and never reset the responses at the correct lever[50]. However, we observed that mice adopted one of two strategies under these training conditions: (1) responding at one lever until sucrose or the timeout consequence was administered, then adjusting responding accordingly (stay or switch), or (2) alternating back and forth between levers, performing 2 to 3 responses at each lever for the entire session. Both strategies relied on external information, as opposed to the interoceptive cues of food deprivation or satiety and did not lead to consistent condition-appropriate responding. The adjustment of not reinforcing or punishing the inactive lever but requiring continuous bouts of responding at the active lever at a high FR schedule (FR15) required the mice to use interoceptive information to commit to one lever or the other and demonstrate reliable stimulus control. Insufficient stimulus control (i.e., performing too many incorrect responses) thus became very clear.

Two generalization tests (one ‘fasted’ and one ‘sated’) were performed following the qualification criteria described above to ensure stimulus control prior to surgery. Mice were placed in the operant chamber for a 10-min habituation period. During the active period, the house light was illuminated but responses at either lever were reinforced with sucrose pellets under the FR15 schedule (each lever had an independent FR15 schedule). Generalization tests lasted until mice earned 5 reinforcers or 20 min elapsed, whichever occurred first. Appropriate discriminative performance for at least two training days (one ‘fasted’ and one ‘sated’) was required between generalization tests. After these initial two generalization tests, stereotaxic surgery was performed.

**Stereotaxic viral injection—**Mice were anesthetized with isoflurane and placed onto a stereotaxic apparatus (David Kopf Instruments, CA, USA). After exposing the skull by a minor incision, small holes (< 1 mm diameter) were drilled bilaterally for virus injection. For all experiments, 50 nl of an adeno-associated virus cocktail was injected bilaterally (rate: 30 nl/min) into the ARC (bregma: −1.70 mm; midline: ±0.25 mm; dorsal skull surface: −5.85, −5.80 and −5.75 mm; $Agrp^{Cre}$ mice) or LH (bregma: −1.23 mm; midline: ±1.00 mm; dorsal skull surface: −5.15 mm; $Vgat^{Cre}$ and $Vglut2^{Cre}$ mice) by a pulled glass pipette (20 – 30 μm tip diameter) with a micromanipulator (Narishige International USA Inc., NY, USA) controlling the injection speed.

One of two viral cocktails was injected: (1) Experimental: rAAV2/9-EF1α-double floxed-hChR2(H134R)-EYFP-WPRE-HGHpA (Addgene viral prep 20298-AAV9) + rAAV2/9-hSyn-DIO-hM4D(Gi)-mCherry (Addgene viral prep 44362-AAV9), or (2) Control: rAAV2/9-EF1α-DIO-EYFP (Addgene viral prep 27056-AAV9) + rAAV2/9-hSyn-DIO-mCherry (Addgene viral prep 50459-AAV9). All viruses were injected at a titer of $5.0 \times 10^{12}$ GC/ml.

For optogenetic targeting of the ARC, optical fibers were implanted unilaterally above the ARC (bregma: −1.70 mm; midline: +0.25 mm; dorsal skull surface: −5.60 mm), and for optogenetic targeting of the LH, optical fibers were implanted bilaterally above the LH (bregma: −1.23 mm; midline: ±1.10 mm, 5° angle; dorsal skull surface: −4.80 mm). Fiber implants were affixed to the skull with cyanoacrylate adhesive and C&B Metabond Quick Adhesive Cement System (Parkell, Inc., NY, USA). Subsequently, mice were given one week for post-surgical recovery before training resumed. Initially, $n = 36$ mice were trained, and surgeries were performed on all mice. However, one *Vglut2*$^{Cre}$ mouse injected with the experimental virus cocktail died during post-operative recovery. This mouse was removed from all Figure 1 analyses. A *Vglut2*$^{Cre}$ mouse injected with the control virus cocktail died following testing on the hunger discrimination paradigm but before the free-access feeding and RTPP studies. Optogenetic and chemogenetic testing did not occur until four weeks post-surgery to allow sufficient viral transduction time.

**Optical manipulations—**Optical fiber implants were coupled to patch cords which were connected to lasers (Doric Lenses Inc., Quebec, Canada) via rotary joints mounted over behavioral testing areas. Laser output was controlled by Doric Neuroscience Studio software (v5.1). For photostimulation experiments, 450-nm laser diodes were used to deliver 5-ms pulses of 10- to 15-mW light. For generalization tests, free-access feeding tests, and gel feeding tests, light pulses were delivered for 1 s (2, 5, 10, or 20 Hz, as indicated) followed by a 3-s break[15], with the sequence repeating for the duration of the test. For real-time place preference experiments, 20-Hz photostimulation was delivered constantly while the mouse occupied the photostimulation-paired area. These photostimulation protocols are commonly used and do not induce significant off-target effects such as heat in brain tissue[64].

**Drugs—**Rimonabant (Cat. No. 9000484), bupropion (Cat. No. 10488), lorcaserin (Cat. No. 15521), liraglutide (Cat. No. 24727), and phentermine (Cat. No. 14207) were purchased from Cayman Chemical (MI, USA); naltrexone hydrochloride (Cat. No. N3136) was purchased from Millipore Sigma (MO, USA), and ghrelin (Cat. No. AS24159) was purchased from Anaspec (CA, USA). Clozapine *N*-oxide (CNO; Cat. No. 4936) was purchased from Tocris Bioscience (Bristol, UK), and lithium chloride (LiCl; Cat. No. L0600) was purchased from Teknova, Inc. (CA, USA). Rimonabant was dissolved in 8% Tween-80 in 0.9% saline and administered subcutaneously (s.c.). Naltrexone and bupropion were combined in a mixture of 1 part per weight naltrexone and 10 parts per weight bupropion, dissolved in saline and administered i.p. lorcaserin, liraglutide, phentermine, ghrelin, and CNO were dissolved in saline and administered i.p., except liraglutide, which was administered s.c. LiCl was diluted in sterile water and administered i.p. All drugs were

prepared freshly the day of use and administered in a volume of 10 ml/kg, except LiCl which was administered in a volume of 30 ml/kg.

**Generalization tests—**Generalization tests were performed to compare the discriminative stimulus effects of $ARC^{AGRP}$, $LH^{VGAT}$, or $LH^{VGLUT2}$ neuronal activation or inhibition to natural states of food deprivation or satiety. Following stereotaxic surgery and recovery, mice continued training until condition-appropriate (>80% correct lever presses) discriminative performance for at least two training days (one 'fasted' and one 'sated') was met before the first generalization test, and this requirement for appropriate responding across two training sessions separated all generalization tests. For 'sated' condition generalization tests, $ARC^{AGRP}$ and $LH^{VGAT}$ experimental mice were tested with the following optogenetic photostimulation protocols: no stim, 2 Hz, 5 Hz, 10 Hz, and 20 Hz; control mice were only tested under no stim and 20 Hz photostimulation. Due to the delay in $ARC^{AGRP}$ photostimulation effects on feeding, $ARC^{AGRP}$ photostimulation began 10 min before the active responding period, whereas $LH^{VGAT}$ photostimulation began concurrently with the start of the active responding period. $LH^{VGLUT2}$ mice received 'sated' generalization tests with inhibitory chemogenetic manipulation, and thus were given 1-hr pretreatments of saline (i.p.) or 1 mg/kg clozapine *N*-oxide (CNO, i.p.). For 'fasted' generalization tests, $ARC^{AGRP}$ and $LH^{VGAT}$ mice were tested with inhibitory chemogenetic manipulations (saline or 1 mg/kg CNO, i.p., 1-hr pretreatment). $LH^{VGLUT2}$ experimental mice were tested with optogenetic photostimulation protocols (no stim, 2 Hz, 5 Hz, 10 Hz, and 20 Hz), which began concurrently with the start of the active period; $LH^{VGLUT2}$ control mice were tested under no stim and 20 Hz photostimulation. All tests were arranged in pseudorandom order.

Following optogenetic and chemogenetic testing in YFP/mCherry control mice, mice were shuffled into three new groups for pharmacological testing to avoid effects of prior testing or genotype. To facilitate data collection, some well-performing mice were used to test more than two compounds and replaced slower, poorly performing mice for these tests. All mice were first given saline treatment prior to control 'fasted' and 'sated' tests to re-verify discriminative control. Six compounds were tested in total, and each group of mice was tested with two compounds. The first group received rimonabant (1 – 10 mg/kg, s.c.) and a mixture of 1-part naltrexone to 10-parts bupropion (0.3 mg/kg naltrexone:3 mg/kg bupropion – 3 mg/kg naltrexone:30 mg/kg bupropion, i.p.) under 'fasted' conditions. The second group received ghrelin (0.3 – 1 mg/kg, i.p.) under 'sated' condition and lorcaserin (1 – 10 mg/kg, i.p.) under 'fasted' condition. The third group received liraglutide (0.03 – 0.3 mg/kg, s.c.) and phentermine (3 – 10 mg/kg, i.p.) under 'fasted' conditions. All compounds were administered 1 h prior to testing, and test orders were arranged pseudorandomly.

Following generalization testing, all mice were housed for 1 week with *ad libitum* access to standard chow in home cages before further behavioral testing.

**Free-access feeding with optogenetics—**Mice were placed into standard rat housing cages that were empty except for one plastic weigh boat secured to the floor that contained 20-mg grain food pellets ("food," Cat. No. 1815928-372; LabDiet) of identical composition to the standard chow (PicoLab Rodent Diet 20) but with different shape and

texture. Tests were 90 min in duration and pellet consumption was assessed at the end of each of 3 consecutive 30-min epochs: pre-photostimulation, photostimulation, and post-photostimulation. *Ad libitum* fed $ARC^{AGRP}$ and $LH^{VGAT}$ experimental and control mice received two of these tests. The first test was performed during the first exposure of the mice to this testing apparatus and food pellets ('novel context'). Then, mice were habituated to the apparatus and food pellets in 1-h sessions across three days before the second test ('habituated').

$LH^{VGLUT2}$ mice were food-restricted and habituated to the context and food source until food intake reliably occurred within 30 min. Then, the food-restricted $LH^{VGLUT2}$ experimental and control mice were given the 90-min optogenetic test described above.

**Free-access feeding with chemogenetics—**Mice were food-restricted for 3 days, with 2-h/day access to standard chow presented on the floor of the home cage, which elicited consistent, large amounts of food intake during tests. For tests, mice were weighed and injected with saline or CNO (1 mg/kg, i.p.) 1 h prior to food delivery. Approximately 5 g of food (1 to 2 pieces of standard chow) was then presented on the floor, and the pellets were collected and weighed at 1, 2, and 4 h post-access. Water was available throughout the test. One $ARC^{AGRP}$:YFP/mCherry mouse was excluded from this test due to malocclusion.

$LH^{VGLUT2}$ experimental and control mice were also tested under *ad libitum* fed conditions as described above. Additional palatable food tests included lard (100% calories from fat; Armour, Conagra Brands, IL, USA), sugar cubes (100% calories from sugar; Domino Sugar, MD, USA), and peanut butter chips (~50% calories from fat, ~40% calories from carbohydrates, ~10% calories from protein; Reese's, The Hershey Company, PA, USA); these tests were separated by at least three days and 1-h CNO pretreatment was always given. Non-caloric gel (orange flavor; Snack Pack, Conagra Brands) tests lasted 1 h, and mice were tested twice on consecutive days, once with CNO pretreatment and once with saline pretreatment conditions. Mice were not habituated to any of these foods prior to the test.

**Real-time place preference—**Real-time place preference tests were performed in apparatuses composed of two identical rectangular chambers connected by a small hallway. A thin layer of fresh rodent bedding covered the entire floor of the apparatus. *Ad libitum* fed mice were connected to patch cords, placed in the hallway section of the apparatus, and then, the test began immediately. ANY-maze video tracking software v5 (Stoelting Co., IL, USA) tracked the location of the mouse throughout the 20-min test and triggered 20-Hz photostimulation when the mouse entered one of the chambers, which was kept constant for all mice. Photostimulation ended when the mouse left the chamber. ANY-maze software was used to analyze the time spent in each chamber and average speed of the mice in each chamber.

**Gel devaluation tests—**Prior to testing, $ARC^{AGRP}$ and $LH^{VGAT}$ experimental and control mice were habituated to non-caloric lemon gel (Jello, Kraft Heinz Company, IL, USA) in home cages for 3 d to reduce neophobia to gel foods. Tests were performed in empty rat cages and gels were presented in plastic weigh boats secured to the floor.

For satiety-induced devaluation, mice received 30-min 'free choice' test sessions over three consecutive days with simultaneous access to 2 – 3 g each of caloric (strawberry flavor; Snack Pack brand) and non-caloric (orange flavor; Snack Pack brand) gels. In the first test, *ad libitum* fed mice were placed in the chamber, and gel intake was determined at the end of 30 min. In the second test, mice were pre-exposed to the caloric gel in the home cage for 1 h prior to the test. In the third test, mice were pre-exposed to the caloric gel in the home cage for 1 h prior to the test and received 20-Hz photostimulation (1-s on, 3-s off) throughout the test.

For sickness-induced devaluation, mice received two 1-h 'forced choice' tests over consecutive days with access to 3 g of either caloric (peach flavor; Jello brand) or non-caloric (cherry flavor; Jello brand) gel. In the first session, mice were placed in the chamber for 1 h with access to caloric gel, then immediately injected with 6.0 mEq/kg LiCl (0.2 M (8.48 mg/ml) LiCl injected at 30 ml/kg, i.p.) to induce gastrointestinal malaise and returned to home cages[77,97]. Gel intake was determined. In the second session, mice were returned to the test chamber with access to caloric gel and received 20-Hz photostimulation (1-s on, 3-s off) for 1 h; gel intake was determined at the end of the session. Mice were given three days of recovery and then this two-day procedure was repeated for the non-caloric gel.

**Open field test—**Open field tests were conducted in 30 × 30-cm clear acrylic arenas with a thin layer of bedding on the chamber floor. Mice naive to the chambers were pretreated with 1 mg/kg CNO (i.p.) and 60 min later were gently placed inside the chambers. Total locomotion, time spent in the center area, and maximum speed over 30 min were measured with ANY-maze video tracking system v5 (Stoelting).

**Histology—**Mice were deeply anesthetized with isoflurane and transcardially perfused with 1x phosphate buffered saline (PBS) followed by 4% paraformaldehyde (PFA) in 1x PBS. Whole brains were removed and post-fixed in 4% PFA until further processing. Samples were cryoprotected in 30% sucrose in 1x PBS, frozen on dry ice, and mounted in Tissue-Tek O.C.T. Compound (Sakura Finetek USA, Inc., CA, USA). Coronal brain sections (50-μm thick) were collected in 1x PBS using a Leica Biosystems CM3050 S cryostat (Wetzlar, Germany). Samples containing ChR2/hM4D were stained with anti-GFP and anti-DsRed for visualization. Briefly, free-floating sections were blocked for 2 h in 1x PBS with 0.03% Triton X-100 and 3% normal goat serum (block solution). Sections were then incubated in a cocktail of primary antibodies in block solution overnight at 4°C (1:1000 each; chicken anti-GFP, Cat. No. GFP-1020, Aves Labs, OR, USA; rabbit anti-DsRed, Cat. No. 632496, Clontech/Takara Bio USA, CA, USA). Sections were washed for 6 × 5 min in 1x PBS before incubating with secondary antibodies in block solution for 2 h (1:500 each; Alexa Fluor 488 goat anti-chicken, Cat. No. A11039; Alexa Fluor 647 goat anti-rabbit, Cat. No. A21245; Invitrogen/Thermo Fisher Scientific, CA, USA). Subsequently, sections were counterstained with DAPI in 1x PBS (1:5000; 4',6-Diamidino-2-Phenylindole, Dilactate; Cat. No. D3571, Invitrogen/Thermo Fisher Scientific) and washed in 1x PBS. Sections were mounted with Fluoromount-G aqueous mounting medium (Electron Microscopy Sciences, PA, USA) onto Superfrost Plus glass slides (VWR International, PA, USA). Images were

taken with an AxioZoom.V16 fluorescence microscope and LSM 700 laser scanning confocal microscope using Zen 2012 software (Carl Zeiss Microscopy LLC, NY, USA).

### Quantification and statistical analyses

Graphs and statistics were generated with Prism 8 software (GraphPad Software, CA, USA). All data are plotted as mean ± s.e.m, and significant effects were noted if $p < 0.05$. Data were analyzed with unpaired Student's t-tests, or one-, two-, or three-way repeated-measures or mixed-model ANOVAs as indicated in the figure legends. Geisser-Greenhouse correction was applied to operant responding data. Dunnett's, Bonferroni's, or Tukey's post-tests were performed following significant ANOVA values to determine pairwise differences between conditions. Sample sizes were chosen based on similar prior experiments that yielded significant results with similar sizes[3,4,49,51].

## Supplementary Material

Refer to Web version on PubMed Central for supplementary material.

## Acknowledgments

The authors acknowledge with gratitude C.R. Lupica and G. Schoenbaum for discussions and comments on the manuscript, and NIDA IRP Visual Media, in particular A. Russell and L. Brick, for brain slice drawings. Mouse clip art was adapted from Openclipart.org (Creative Commons CC0). M.A.A. was supported by the NIDA IRP Scientific Director's Fellowship for Diversity in Research. This work was supported by the National Institute on Drug Abuse Intramural Research Program (NIDA IRP), U.S. National Institutes of Health (NIH).

## References

1. Rossi MA, and Stuber GD (2018). Overlapping Brain Circuits for Homeostatic and Hedonic Feeding. Cell metabolism 27, 42–56. 10.1016/j.cmet.2017.09.021. [PubMed: 29107504]
2. Ferrario CR, Labouebe G, Liu S, Nieh EH, Routh VH, Xu S, and O'Connor EC (2016). Homeostasis Meets Motivation in the Battle to Control Food Intake. The Journal of neuroscience : the official journal of the Society for Neuroscience 36, 11469–11481. 10.1523/JNEUROSCI.2338-16.2016.
3. Jennings JH, Ung RL, Resendez SL, Stamatakis AM, Taylor JG, Huang J, Veleta K, Kantak PA, Aita M, Shilling-Scrivo K, et al. (2015). Visualizing hypothalamic network dynamics for appetitive and consummatory behaviors. Cell 160, 516–527. 10.1016/j.cell.2014.12.026. [PubMed: 25635459]
4. Jennings JH, Rizzi G, Stamatakis AM, Ung RL, and Stuber GD (2013). The inhibitory circuit architecture of the lateral hypothalamus orchestrates feeding. Science (New York, N.Y.) 341, 1517–1521. 10.1126/science.1241812.
5. Tan KR, Yvon C, Turiault M, Mirzabekov JJ, Doehner J, Labouebe G, Deisseroth K, Tye KM, and Luscher C (2012). GABA neurons of the VTA drive conditioned place aversion. Neuron 73, 1173–1183. 10.1016/j.neuron.2012.02.015.. [PubMed: 22445344]
6. van Zessen R, Phillips JL, Budygin EA, and Stuber GD (2012). Activation of VTA GABA neurons disrupts reward consumption. Neuron 73, 1184–1194. 10.1016/j.neuron.2012.02.016. [PubMed: 22445345]
7. Adamantidis AR, Tsai HC, Boutrel B, Zhang F, Stuber GD, Budygin EA, Tourino C, Bonci A, Deisseroth K, and de Lecea L (2011). Optogenetic interrogation of dopaminergic modulation of the multiple phases of reward-seeking behavior. The Journal of neuroscience : the official journal of the Society for Neuroscience 31, 10829–10835. 10.1523/JNEUROSCI.2246-11.2011.
8. Chen Y, Lin YC, Zimmerman CA, Essner RA, and Knight ZA (2016). Hunger neurons drive feeding through a sustained, positive reinforcement signal. eLife 5. 10.7554/eLife.18640.

9. Fu O, Iwai Y, Narukawa M, Ishikawa AW, Ishii KK, Murata K, Yoshimura Y, Touhara K, Misaka T, Minokoshi Y, and Nakajima KI (2019). Hypothalamic neuronal circuits regulating hunger-induced taste modification. Nature communications 10, 4560. 10.1038/s41467-019-12478-x.
10. Betley JN, Xu S, Cao ZFH, Gong R, Magnus CJ, Yu Y, and Sternson SM (2015). Neurons for hunger and thirst transmit a negative-valence teaching signal. Nature 521, 180–185. 10.1038/nature14416. [PubMed: 25915020]
11. Burnett CJ, Li C, Webber E, Tsaousidou E, Xue SY, Bruning JC, and Krashes MJ (2016). Hunger-Driven Motivational State Competition. Neuron 92, 187–201. 10.1016/j.neuron.2016.08.032. [PubMed: 27693254]
12. Krashes MJ, Shah BP, Madara JC, Olson DP, Strochlic DE, Garfield AS, Vong L, Pei H, Watabe-Uchida M, Uchida N, et al. (2014). An excitatory paraventricular nucleus to AgRP neuron circuit that drives hunger. Nature 507, 238–242. 10.1038/nature12956. [PubMed: 24487620]
13. Atasoy D, Betley JN, Su HH, and Sternson SM (2012). Deconstruction of a neural circuit for hunger. Nature 488, 172–177. 10.1038/nature11270. [PubMed: 22801496]
14. Beutler LR, Chen Y, Ahn JS, Lin YC, Essner RA, and Knight ZA (2017). Dynamics of Gut-Brain Communication Underlying Hunger. Neuron 96, 461–475 e465. 10.1016/j.neuron.2017.09.043. [PubMed: 29024666]
15. Aponte Y, Atasoy D, and Sternson SM (2011). AGRP neurons are sufficient to orchestrate feeding behavior rapidly and without training. Nature neuroscience 14, 351–355. 10.1038/nn.2739. [PubMed: 21209617]
16. Mazzone CM, Liang-Guallpa J, Li C, Wolcott NS, Boone MH, Southern M, Kobzar NP, Salgado IA, Reddy DM, Sun F, et al. (2020). High-fat food biases hypothalamic and mesolimbic expression of consummatory drives. Nature neuroscience 23, 1253–1266. 10.1038/s41593-020-0684-9. [PubMed: 32747789]
17. Chen Y, Lin YC, Kuo TW, and Knight ZA (2015). Sensory detection of food rapidly modulates arcuate feeding circuits. Cell 160, 829–841. 10.1016/j.cell.2015.01.033. [PubMed: 25703096]
18. Su Z, Alhadeff AL, and Betley JN (2017). Nutritive, Post-ingestive Signals Are the Primary Regulators of AgRP Neuron Activity. Cell reports 21, 2724–2736. 10.1016/j.celrep.2017.11.036. [PubMed: 29212021]
19. Mandelblat-Cerf Y, Ramesh RN, Burgess CR, Patella P, Yang Z, Lowell BB, and Andermann ML (2015). Arcuate hypothalamic AgRP and putative POMC neurons show opposite changes in spiking across multiple timescales. eLife 4, e07122. 10.7554/eLife.07122.
20. Livneh Y, Sugden AU, Madara JC, Essner RA, Flores VI, Sugden LA, Resch JM, Lowell BB, and Andermann ML (2020). Estimation of Current and Future Physiological States in Insular Cortex. Neuron 105, 1094–1111 e1010. 10.1016/j.neuron.2019.12.027. [PubMed: 31955944]
21. Livneh Y, Ramesh RN, Burgess CR, Levandowski KM, Madara JC, Fenselau H, Goldey GJ, Diaz VE, Jikomes N, Resch JM, et al. (2017). Homeostatic circuits selectively gate food cue responses in insular cortex. Nature 546, 611–616. 10.1038/nature22375. [PubMed: 28614299]
22. Li C, Hou Y, Zhang J, Sui G, Du X, Licinio J, Wong ML, and Yang Y (2019). AGRP neurons modulate fasting-induced anxiolytic effects. Transl Psychiatry 9, 111. 10.1038/s41398-019-0438-1. [PubMed: 30850579]
23. Alhadeff AL, Su Z, Hernandez E, Klima ML, Phillips SZ, Holland RA, Guo C, Hantman AW, De Jonghe BC, and Betley JN (2018). A Neural Circuit for the Suppression of Pain by a Competing Need State. Cell 173, 140–152 e115. 10.1016/j.cell.2018.02.057. [PubMed: 29570993]
24. Essner RA, Smith AG, Jamnik AA, Ryba AR, Trutner ZD, and Carter ME (2017). AgRP Neurons Can Increase Food Intake during Conditions of Appetite Suppression and Inhibit Anorexigenic Parabrachial Neurons. The Journal of neuroscience : the official journal of the Society for Neuroscience 37, 8678–8687. 10.1523/JNEUROSCI.0798-17.2017. [PubMed: 28821663]
25. Krashes MJ, Koda S, Ye C, Rogan SC, Adams AC, Cusher DS, Maratos-Flier E, Roth BL, and Lowell BB (2011). Rapid, reversible activation of AgRP neurons drives feeding behavior in mice. The Journal of clinical investigation 121, 1424–1428. 10.1172/JCI46229. [PubMed: 21364278]
26. Alhadeff AL, Goldstein N, Park O, Klima ML, Vargas A, and Betley JN (2019). Natural and Drug Rewards Engage Distinct Pathways that Converge on Coordinated Hypothalamic and Reward Circuits. Neuron 103, 891–908.e896. 10.1016/j.neuron.2019.05.050. [PubMed: 31277924]

27. Wise RA (1974). Lateral hypothalamic electrical stimulation: does it make animals 'hungry'? Brain research 67, 187–209. 10.1016/0006-8993(74)90272-8. [PubMed: 4620218]
28. Gosnell BA, and Krahn DD (1993). Morphine-induced feeding: a comparison of the Lewis and Fischer 344 inbred rat strains. Pharmacology, biochemistry, and behavior 44, 919–924. 10.1016/0091-3057(93)90025-o.
29. Miller NE (1960). Motivational effects of brain stimulation and drugs. Federation proceedings 19, 846–854. [PubMed: 13770870]
30. Jacobs BL, and Farel PB (1971). Motivated behaviors produced by increased arousal in the presence of goal objects. Physiology & behavior 6, 473–476. 10.1016/0031-9384(71)90191-0. [PubMed: 5170001]
31. Barnett SA (1958). Experiments on neophobia in wild and laboratory rats. Br J Psychol 49, 195–201. 10.1111/j.2044-8295.1958.tb00657.x. [PubMed: 13572791]
32. Barnett SA, and Spencer MM (1953). Responses of wild rats to offensive smells and tastes. The British Journal of Animal Behaviour 1, 32–37. 10.1016/s0950-5601(53)80084-5.
33. Ghent L (1957). Some effects of deprivation of eating and drinking behavior. J Comp Physiol Psychol 50, 172–176. 10.1037/h0042629. [PubMed: 13449201]
34. Klenotich SJ, and Dulawa SC (2012). The activity-based anorexia mouse model. Methods in molecular biology (Clifton, N.J.) 829, 377–393. 10.1007/978-1-61779-458-2_25.
35. Samuels BA, and Hen R (2011). Novelty-Suppressed Feeding in the Mouse. In Mood and Anxiety Related Phenotypes in Mice, Gould TD, ed. (Humana Press), pp. 107–121. 10.1007/978-1-61779-313-4_7.
36. Valenstein ES, Cox VC, and Kakolewski JW (1968). The motivation underlying eating elicited by lateral hypothalamic stimulation. Physiology & behavior 3, 969–971. 10.1016/0031-9384(68)90185-6.
37. Dietrich MO, Zimmer MR, Bober J, and Horvath TL (2015). Hypothalamic Agrp neurons drive stereotypic behaviors beyond feeding. Cell 160, 1222–1232. 10.1016/j.cell.2015.02.024. [PubMed: 25748653]
38. Bolin BL, Alcorn JL, Reynolds AR, Lile JA, and Rush CR (2016). Human drug discrimination: A primer and methodological review. Exp Clin Psychopharmacol 24, 214–228. 10.1037/pha0000077. [PubMed: 27454673]
39. Porter JH, and Prus AJ (2009). Drug discrimination: 30 years of progress. Psychopharmacology 203, 189–191. 10.1007/s00213-009-1478-7. [PubMed: 19225764]
40. Walker DM, Cates HM, Loh YE, Purushothaman I, Ramakrishnan A, Cahill KM, Lardner CK, Godino A, Kronman HG, Rabkin J, et al. (2018). Cocaine Self-administration Alters Transcriptome-wide Responses in the Brain's Reward Circuitry. Biological psychiatry 84, 867–880. 10.1016/j.biopsych.2018.04.009. [PubMed: 29861096]
41. Conrad KL, Tseng KY, Uejima JL, Reimers JM, Heng LJ, Shaham Y, Marinelli M, and Wolf ME (2008). Formation of accumbens GluR2-lacking AMPA receptors mediates incubation of cocaine craving. Nature 454, 118–121. 10.1038/nature06995. [PubMed: 18500330]
42. Towers EB, Tunstall BJ, McCracken ML, Vendruscolo LF, and Koob GF (2019). Male and female mice develop escalation of heroin intake and dependence following extended access. Neuropharmacology 151, 189–194. 10.1016/j.neuropharm.2019.03.019. [PubMed: 30880124]
43. Venniro M, Russell TI, Zhang M, and Shaham Y (2019). Operant Social Reward Decreases Incubation of Heroin Craving in Male and Female Rats. Biological psychiatry 86, 848–856. 10.1016/j.biopsych.2019.05.018.. [PubMed: 31326085]
44. Lamas X, Negus SS, Gatch MB, and Mello NK (1998). Effects of heroin/cocaine combinations in rats trained to discriminate heroin or cocaine from saline. Pharmacology, biochemistry, and behavior 60, 357–364. 10.1016/s0091-3057(98)00021-5.
45. Woolfolk DR, and Holtzman SG (1997). μ-, δ- and κ-opioid receptor agonists do not alter the discriminative stimulus effects of cocaine or d-amphetamine in rats. Drug and Alcohol Dependence 48, 209–220. 10.1016/s0376-8716(97)00129-4. [PubMed: 9449020]
46. Schuh KJ, Schaal DW, Thompson T, Cleary JP, Billington CJ, and Levine AS (1994). Insulin, 2-deoxy-D-glucose, and food deprivation as discriminative stimuli in rats. Pharmacology, biochemistry, and behavior 47, 317–324. 10.1016/0091-3057(94)90016-7.

47. Corwin RL, Woolverton WL, and Schuster CR (1990). Effects of cholecystokinin, d-amphetamine and fenfluramine in rats trained to discriminate 3 from 22 hr of food deprivation. The Journal of pharmacology and experimental therapeutics 253, 720–728. [PubMed: 2338655]
48. Sample CH, Jones S, Dwider F, and Davidson TL (2018). Discriminative control by deprivation states and external cues in male and female rats. Physiology & behavior 184, 91–99. 10.1016/j.physbeh.2017.08.019. [PubMed: 28847483]
49. Jewett DC, Lefever TW, Flashinski DP, Koffarnus MN, Cameron CR, Hehli DJ, Grace MK, and Levine AS (2006). Intraparaventricular neuropeptide Y and ghrelin induce learned behaviors that report food deprivation in rats. Neuroreport 17, 733–737. 10.1097/01.wnr.0000215767.94528.fb. [PubMed: 16641678]
50. Jewett DC, Hahn TW, Smith TR, Fiksdal BL, Wiebelhaus JM, Dunbar AR, Filtz CR, Novinska NL, and Levine AS (2009). Effects of sibutramine and rimonabant in rats trained to discriminate between 22- and 2-h food deprivation. Psychopharmacology 203, 453–459. 10.1007/s00213-008-1350-1. [PubMed: 18854986]
51. Jewett DC, Klockars A, Smith TR, Brunton C, Head MA, Tham RL, Kwilasz AJ, Hahn TW, Wiebelhaus JM, Ewan EE, et al. (2020). Effects of opioid receptor ligands in rats trained to discriminate 22 from 2 hours of food deprivation suggest a lack of opioid involvement in eating for hunger. Behavioural brain research 380, 112369. 10.1016/j.bbr.2019.112369. [PubMed: 31743731]
52. Head MA, Jewett DC, Gartner SN, Klockars A, Levine AS, and Olszewski PK (2019). Effect of Oxytocin on Hunger Discrimination. Frontiers in endocrinology 10, 297. 10.3389/fendo.2019.00297. [PubMed: 31156549]
53. Solinas M, Panlilio LV, Justinova Z, Yasar S, and Goldberg SR (2006). Using drug-discrimination techniques to study the abuse-related effects of psychoactive drugs in rats. Nat Protoc 1, 1194–1206. 10.1038/nprot.2006.167. [PubMed: 17406402]
54. Li JX, Koek W, Rice KC, and France CP (2010). Differential effects of serotonin 5-HT1A receptor agonists on the discriminative stimulus effects of the 5-HT2A receptor agonist 1-(2,5-dimethoxy-4-methylphenyl)-2-aminopropane in rats and rhesus monkeys. The Journal of pharmacology and experimental therapeutics 333, 244–252. 10.1124/jpet.109.163451. [PubMed: 20053932]
55. Li JX, Shah AP, Patel SK, Rice KC, and France CP (2013). Modification of the behavioral effects of morphine in rats by serotonin (5-HT) (1A) and 5-HT(2) receptor agonists: antinociception, drug discrimination, and locomotor activity. Psychopharmacology 225, 791–801. [PubMed: 22993050]
56. Siemian JN, Wang K, Zhang Y, and Li JX (2018). Mechanisms of imidazoline I2 receptor agonist-induced antinociception in rats: involvement of monoaminergic neurotransmission. British journal of pharmacology 175, 1519–1534. 10.1111/bph.14161. [PubMed: 29451703]
57. Collins GT, Jackson JA, Koek W, and France CP (2014). Effects of dopamine D(2)-like receptor agonists in mice trained to discriminate cocaine from saline: influence of feeding condition. Eur J Pharmacol 729, 123–131. 10.1016/j.ejphar.2014.02.014. [PubMed: 24561049]
58. Tong Q, Ye CP, Jones JE, Elmquist JK, and Lowell BB (2008). Synaptic release of GABA by AgRP neurons is required for normal regulation of energy balance. Nature neuroscience 11, 998–1000. 10.1038/nn.2167. [PubMed: 19160495]
59. Kaelin CB, Xu AW, Lu XY, and Barsh GS (2004). Transcriptional regulation of agouti-related protein (Agrp) in transgenic mice. Endocrinology 145, 5798–5806. 10.1210/en.2004-0956. [PubMed: 15345681]
60. Vong L, Ye C, Yang Z, Choi B, Chua S Jr., and Lowell BB (2011). Leptin action on GABAergic neurons prevents obesity and reduces inhibitory tone to POMC neurons. Neuron 71, 142–154. 10.1016/j.neuron.2011.05.028. [PubMed: 21745644]
61. Stachniak TJ, Ghosh A, and Sternson SM (2014). Chemogenetic synaptic silencing of neural circuits localizes a hypothalamus-->midbrain pathway for feeding behavior. Neuron 82, 797–808. 10.1016/j.neuron.2014.04.008. [PubMed: 24768300]
62. Mahn M, Prigge M, Ron S, Levy R, and Yizhar O (2016). Biophysical constraints of optogenetic inhibition at presynaptic terminals. Nature neuroscience 19, 554–556. 10.1038/nn.4266. [PubMed: 26950004]

63. Gomez JL, Bonaventura J, Lesniak W, Mathews WB, Sysa-Shah P, Rodriguez LA, Ellis RJ, Richie CT, Harvey BK, Dannals RF, et al. (2017). Chemogenetics revealed: DREADD occupancy and activation via converted clozapine. Science (New York, N.Y.) 357, 503–507. 10.1126/science.aan2475.
64. Owen SF, Liu MH, and Kreitzer AC (2019). Thermal constraints on in vivo optogenetic manipulations. Nature neuroscience 22, 1061–1065. 10.1038/s41593-019-0422-3. [PubMed: 31209378]
65. Rowland NE, Lo J, and Robertson K (2001). Acute anorectic effect of single and combined drugs in mice using a non-deprivation protocol. Psychopharmacology 157, 193–196. 10.1007/s002130100789. [PubMed: 11594445]
66. Wiley JL, Burston JJ, Leggett DC, Alekseeva OO, Razdan RK, Mahadevan A, and Martin BR (2005). CB1 cannabinoid receptor-mediated modulation of food intake in mice. British journal of pharmacology 145, 293–300. 10.1038/sj.bjp.0706157. [PubMed: 15778743]
67. Greenway FL, Whitehouse MJ, Guttadauria M, Anderson JW, Atkinson RL, Fujioka K, Gadde KM, Gupta AK, O'Neil P, Schumacher D, et al. (2009). Rational design of a combination medication for the treatment of obesity. Obesity (Silver Spring, Md.) 17, 30–39. 10.1038/oby.2008.461.
68. Grottick AJ, Whelan K, Sanabria EK, Behan DP, Morgan M, and Sage C (2015). Investigating interactions between phentermine, dexfenfluramine, and 5-HT2C agonists, on food intake in the rat. Psychopharmacology 232, 1973–1982. 10.1007/s00213-014-3829-2. [PubMed: 25524140]
69. Fletcher PJ, Tampakeras M, Sinyard J, Slassi A, Isaac M, and Higgins GA (2009). Characterizing the effects of 5-HT(2C) receptor ligands on motor activity and feeding behaviour in 5-HT(2C) receptor knockout mice. Neuropharmacology 57, 259–267. 10.1016/j.neuropharm.2009.05.011. [PubMed: 19501602]
70. Sisley S, Gutierrez-Aguilar R, Scott M, D'Alessio DA, Sandoval DA, and Seeley RJ (2014). Neuronal GLP1R mediates liraglutide's anorectic but not glucose-lowering effect. The Journal of clinical investigation 124, 2456–2463. 10.1172/JCI72434. [PubMed: 24762441]
71. Coulter AA, Rebello CJ, and Greenway FL (2018). Centrally Acting Agents for Obesity: Past, Present, and Future. Drugs 78, 1113–1132. 10.1007/s40265-018-0946-y. [PubMed: 30014268]
72. Srivastava G, and Apovian CM (2018). Current pharmacotherapy for obesity. Nature reviews. Endocrinology 14, 12–24. 10.1038/nrendo.2017.122. [PubMed: 29027993]
73. Bachmanov AA, Tordoff MG, and Beauchamp GK (2001). Sweetener preference of C57BL/6ByJ and 129P3/J mice. Chemical senses 26, 905–913. 10.1093/chemse/26.7.905. [PubMed: 11555485]
74. Gardner MPH, Conroy JS, Shaham MH, Styer CV, and Schoenbaum G (2017). Lateral Orbitofrontal Inactivation Dissociates Devaluation-Sensitive Behavior and Economic Choice. Neuron 96, 1192–1203 e1194. 10.1016/j.neuron.2017.10.026. [PubMed: 29154127]
75. Wise RA, and Albin J (1973). Stimulation-induced eating disrupted by a conditioned taste aversion. Behavioral biology 9, 289–297. 10.1016/s0091-6773(73)80179-8. [PubMed: 4743422]
76. Miller V, and Domjan M (1981). Selective sensitization induced by lithium malaise and footshock in rats. Behavioral and neural biology 31, 42–55. 10.1016/s0163-1047(81)91050-5. [PubMed: 6272678]
77. Ingram DK (1982). Lithium chloride-induced taste aversion in C57BL/6J and DBA/2J mice. The Journal of general psychology 106, 233–249.
78. Saunders A, Johnson CA, and Sabatini BL (2012). Novel recombinant adeno-associated viruses for Cre activated and inactivated transgene expression in neurons. Front Neural Circuits 6, 47. 10.3389/fncir.2012.00047. [PubMed: 22866029]
79. Jennings JH, Kim CK, Marshel JH, Raffiee M, Ye L, Quirin S, Pak S, Ramakrishnan C, and Deisseroth K (2019). Interacting neural ensembles in orbitofrontal cortex for social and feeding behaviour. Nature 565, 645–649. 10.1038/s41586-018-0866-8. [PubMed: 30651638]
80. Alves S, Bode J, Bemelmans AP, von Kalle C, Cartier N, and Tews B (2016). Ultramicroscopy as a novel tool to unravel the tropism of AAV gene therapy vectors in the brain. Scientific reports 6, 28272. 10.1038/srep28272. [PubMed: 27320056]

81. Dodd GT, Kim SJ, Méquinion M, Xirouchaki CE, Brüning JC, Andrews ZB, and Tiganis T (2021). Insulin signaling in AgRP neurons regulates meal size to limit glucose excursions and insulin resistance. Sci Adv 7. 10.1126/sciadv.abf4100.
82. Reichenbach A, Stark R, Mequinion M, Lockie SH, Lemus MB, Mynatt RL, Luquet S, and Andrews ZB (2018). Carnitine acetyltransferase (Crat) in hunger-sensing AgRP neurons permits adaptation to calorie restriction. Faseb j 32, fj201800634R. 10.1096/fj.201800634R.
83. Reichenbach A, Stark R, Mequinion M, Denis RRG, Goularte JF, Clarke RE, Lockie SH, Lemus MB, Kowalski GM, Bruce CR, et al. (2018). AgRP Neurons Require Carnitine Acetyltransferase to Regulate Metabolic Flexibility and Peripheral Nutrient Partitioning. Cell reports 22, 1745–1759. 10.1016/j.celrep.2018.01.067. [PubMed: 29444428]
84. Chen Y, Essner RA, Kosar S, Miller OH, Lin YC, Mesgarzadeh S, and Knight ZA (2019). Sustained NPY signaling enables AgRP neurons to drive feeding. eLife 8. 10.7554/eLife.46348.
85. Beutler LR, Corpuz TV, Ahn JS, Kosar S, Song W, Chen Y, and Knight ZA (2020). Obesity causes selective and long-lasting desensitization of AgRP neurons to dietary fat. eLife 9, e55909. 10.7554/eLife.55909. [PubMed: 32720646]
86. de Araujo IE, Oliveira-Maia AJ, Sotnikova TD, Gainetdinov RR, Caron MG, Nicolelis MAL, and Simon SA (2008). Food Reward in the Absence of Taste Receptor Signaling. Neuron 57, 930–941. 10.1016/j.neuron.2008.01.032. [PubMed: 18367093]
87. Nieh EH, Vander Weele CM, Matthews GA, Presbrey KN, Wichmann R, Leppla CA, Izadmehr EM, and Tye KM (2016). Inhibitory Input from the Lateral Hypothalamus to the Ventral Tegmental Area Disinhibits Dopamine Neurons and Promotes Behavioral Activation. Neuron 90, 1286–1298. 10.1016/j.neuron.2016.04.035. [PubMed: 27238864]
88. Rossi MA, Basiri ML, McHenry JA, Kosyk O, Otis JM, van den Munkhof HE, Bryois J, Hubel C, Breen G, Guo W, et al. (2019). Obesity remodels activity and transcriptional state of a lateral hypothalamic brake on feeding. Science (New York, N.Y.) 364, 1271–1274. 10.1126/science.aax1184.
89. Stamatakis AM, Van Swieten M, Basiri ML, Blair GA, Kantak P, and Stuber GD (2016). Lateral Hypothalamic Area Glutamatergic Neurons and Their Projections to the Lateral Habenula Regulate Feeding and Reward. The Journal of neuroscience : the official journal of the Society for Neuroscience 36, 302–311. 10.1523/JNEUROSCI.1202-15.2016.
90. Garau C, Blomeley C, and Burdakov D (2020). Orexin neurons and inhibitory Agrp→orexin circuits guide spatial exploration in mice. The Journal of physiology 598, 4371–4383. 10.1113/jp280158. [PubMed: 32667686]
91. Bonnavion P, Mickelsen LE, Fujita A, de Lecea L, and Jackson AC (2016). Hubs and spokes of the lateral hypothalamus: cell types, circuits and behaviour. The Journal of physiology 594, 6443–6462. 10.1113/JP271946. [PubMed: 27302606]
92. Wang C, Zhou W, He Y, Yang T, Xu P, Yang Y, Cai X, Wang J, Liu H, Yu M, et al. (2021). AgRP neurons trigger long-term potentiation and facilitate food seeking. Translational psychiatry 11, 11. 10.1038/s41398-020-01161-1. [PubMed: 33414382]
93. Betley JN, Cao ZF, Ritola KD, and Sternson SM (2013). Parallel, redundant circuit organization for homeostatic control of feeding behavior. Cell 155, 1337–1350. 10.1016/j.cell.2013.11.002. [PubMed: 24315102]
94. Steculorum SM, Ruud J, Karakasilioti I, Backes H, Engström Ruud L, Timper K, Hess ME, Tsaousidou E, Mauer J, Vogt MC, et al. (2016). AgRP Neurons Control Systemic Insulin Sensitivity via Myostatin Expression in Brown Adipose Tissue. Cell 165, 125–138. 10.1016/j.cell.2016.02.044. [PubMed: 27015310]
95. Craig AD (2009). How do you feel--now? The anterior insula and human awareness. Nature reviews. Neuroscience 10, 59–70. 10.1038/nrn2555.
96. Strigo IA, and Craig AD (2016). Interoception, homeostatic emotions and sympathovagal balance. Philos Trans R Soc Lond B Biol Sci 371. 10.1098/rstb.2016.0010.
97. Kislal S, and Blizard DA (2016). Conditioned context aversion learning in the laboratory mouse. Learn Behav 44, 309–319. 10.3758/s13420-016-0217-2. [PubMed: 26961783]

## Highlights

- Mice can be trained to report periods of fasting from satiety
- In sated mice, $ARC^{AGRP}$ neuronal activation evoked fasted-associated responding
- In fasted mice, $LH^{VGAT}$ inhibition or $LH^{VGLUT2}$ activation drove satiety-like effects
- Only $ARC^{AGRP}$ neuronal activation drove calorie-specific feeding

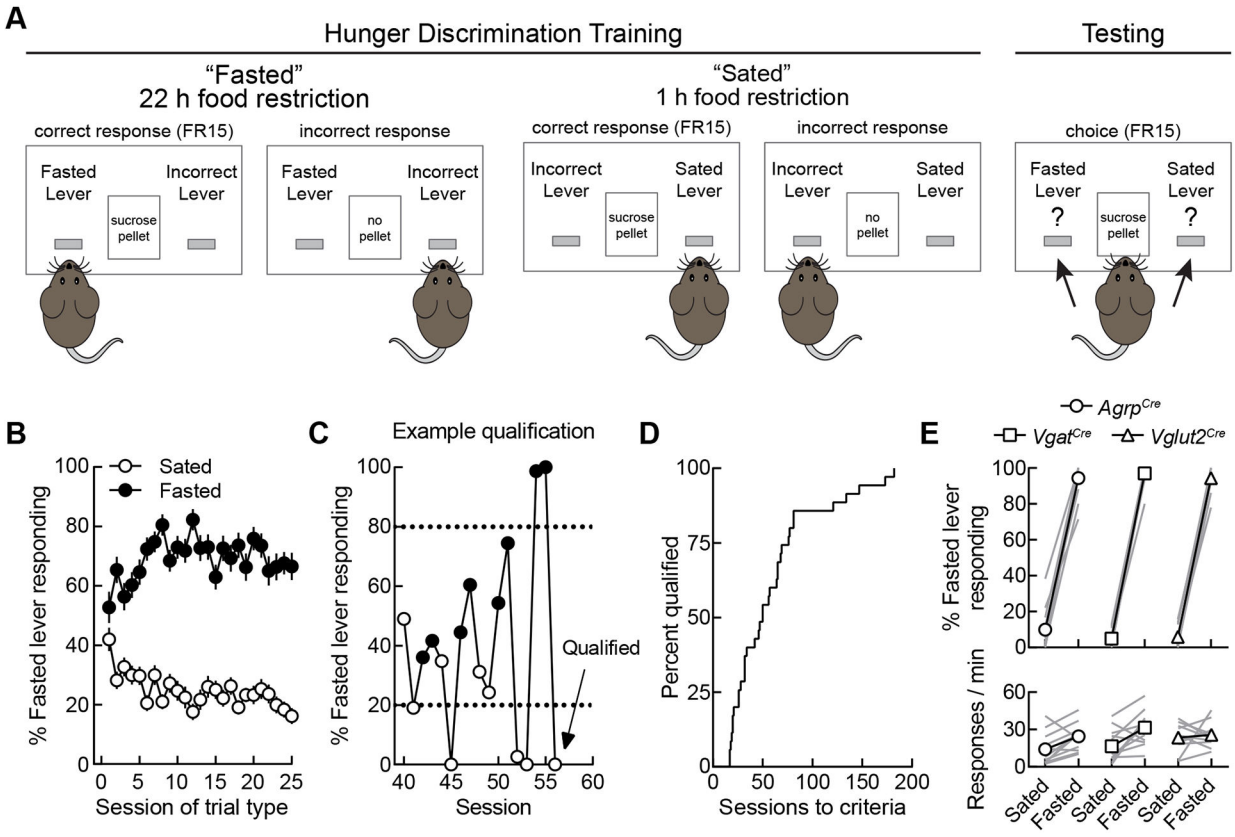


**Figure 1. Discriminative control by feeding condition in mice.**

(**A**) Schematic of the operant hunger discrimination paradigm. During training sessions, responses on one designated active lever depending on feeding condition were reinforced (e.g., 22-h food-restricted, left lever active; 1-h food-restricted, right lever active) with sucrose pellets on an FR15 schedule, whereas responses on the opposite lever reset active lever requirements. During testing sessions, responses on both levers were reinforced. All sessions lasted for 20 min or until five pellets were earned.

(**B**) Group-averaged data for all mice ($n = 35$) on the first 25 sessions of each trial type. Condition-appropriate responding increased as training progressed.

(**C**) Mice qualified for training by performing >80% responses on the condition-appropriate lever (shown as dotted lines) for five consecutive sessions or six out of seven consecutive sessions. This graph shows training data from a representative mouse during training sessions 40 through 56. On sessions 51 through 56, the mouse exceeded the 80% threshold each session and qualified for testing.

(**D**) Acquisition curve depicting the number of sessions required for each mouse to reach training criteria. ($n = 35$ mice)

(**E**) Performance of mice during free-choice test sessions ($n = 12$ $Agrp^{Cre}$ mice, 12 $Vgat^{Cre}$ mice, and 11 $Vglut2^{Cre}$ mice). *Upper panels*, condition-appropriate lever responding; *lower panels*, response rate.

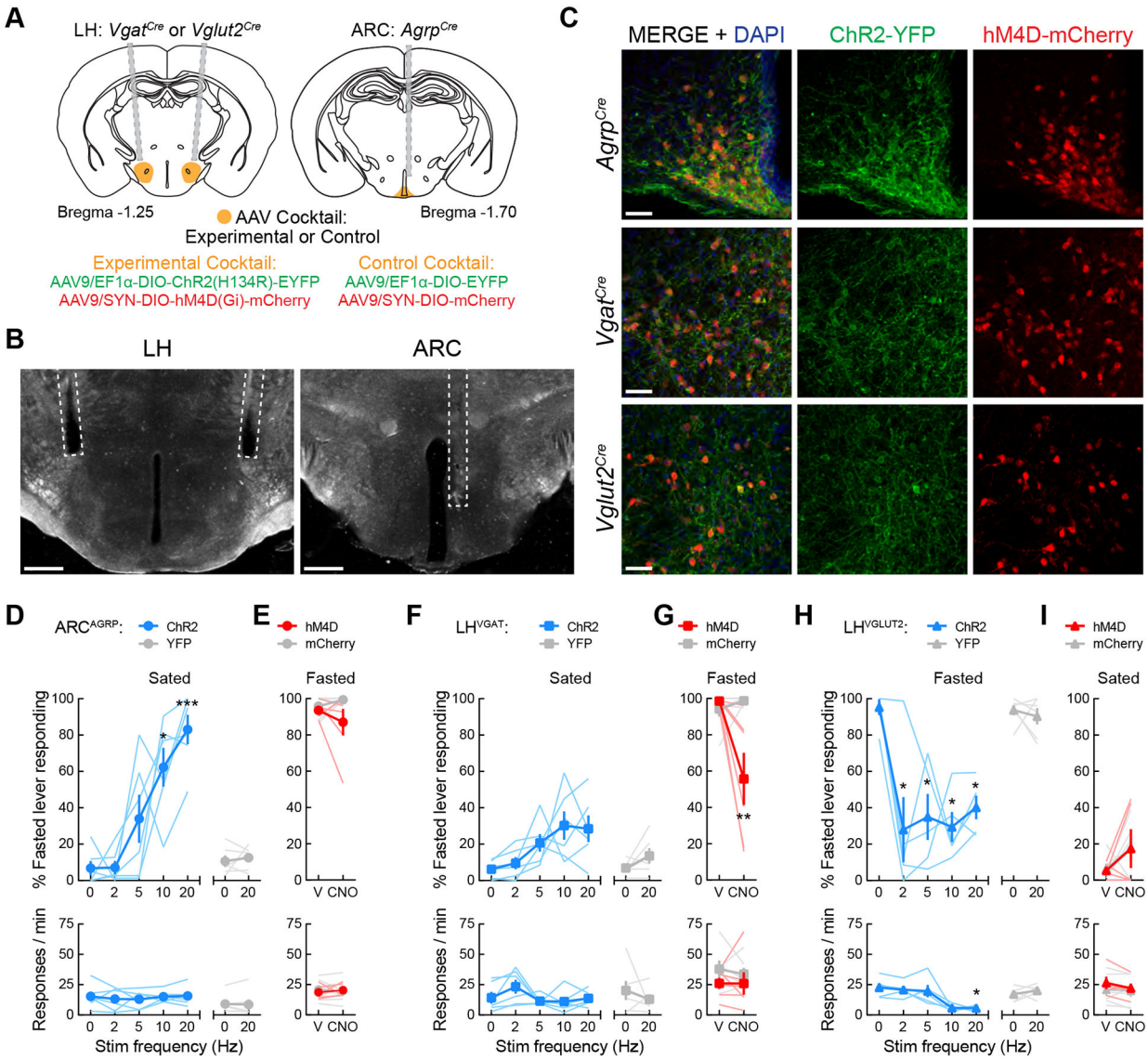


**Figure 2. Hypothalamic control of hunger- and satiety-associated interoceptive cues.**

(**A**) Surgery schematic for experimental and control viral cocktail injections into the ARC of *Agrp*$^{Cre}$ mice or the LH of *Vgat*$^{Cre}$ and *Vglut2*$^{Cre}$ mice.

(**B**) Representative images showing optical fiber placement in the ARC of *Agrp*$^{Cre}$ mice or in the LH of *Vgat*$^{Cre}$ and *Vglut2*$^{Cre}$ mice. Scale bar = 500 μm.

(**C**) 20× confocal images demonstrating colocalization of ChR2-YFP (green) and hM4D-mCherry (red) in the ARC of *Agrp*$^{Cre}$ mice and in the LH of *Vgat*$^{Cre}$ and *Vglut2*$^{Cre}$ mice. Scale bar = 50 μm.

(**D**) ARC$^{AGRP}$ activation in sated mice triggers hunger. *Upper panel*, one-way repeated-measures ANOVA revealed a significant effect of photostimulation in ARC$^{AGRP}$:ChR2 mice ($n$ = 6; $F$(1.62, 8.11) = 14.12, $p$ = 0.003; Dunnett's post-test: no stim vs. 10 Hz,*$p$ = 0.022; no stim vs. 20 Hz, ***$p$ = 0.001) on fasted-associated lever responding. No significant effects were observed in YFP controls ($n$ = 6; paired t test: $t$(5) = 0.53, $p$ = 0.62). *Lower*

*panel*, no effects of photostimulation on response rate were observed in $ARC^{AGRP}$:ChR2 ($F(1.98, 9.92) = 0.29$, $p = 0.75$) or $ARC^{AGRP}$:YFP mice ($t(5) = 0.37$, $p = 0.73$).

(**E**) $ARC^{AGRP}$ inhibition in fasted mice does not decrease hunger. *Upper panel*, two-way mixed-model ANOVA found no significant effects of $ARC^{AGRP}$ inhibition on fasted-associated lever responding ($n = 6$ mice per group; group × treatment interaction: $F(1, 10) = 1.81$, $p = 0.21$) or response rate (*lower panel*, $F(1, 10) = 0.70$, $p = 0.42$).

(**F**) $LH^{VGAT}$ activation in sated mice does not evoke hunger. *Upper panel*, no significant effects of photostimulation in $LH^{VGAT}$:ChR2 mice ($n = 6$; $F(1.71, 8.56) = 4.32$, $p = 0.055$) or $LH^{VGAT}$:YFP mice ($n = 6$; $t(5) = 1.61$, $p = 0.17$) were observed. *Lower panel*, no effects of photostimulation on response rate were observed in $LH^{VGAT}$:ChR2 ($F(2.39, 11.95) = 2.59$, $p = 0.11$) or $LH^{VGAT}$:YFP mice ($t(5) = 0.82$, $p = 0.45$).

(**G**) $LH^{VGAT}$ inhibition in fasted mice decreases hunger. *Upper panel*, two-way mixed-model ANOVA found a significant effect of $LH^{VGAT}$ inhibition on fasted-associated lever responding ($n = 6$ mice per group; group × treatment interaction: $F(1, 10) = 10.47$, $p = 0.0089$; Bonferroni's post-test $^{**}p = 0.0013$). *Lower panel*, no effects of inhibition were observed on response rate ($F(1, 10) = 0.18$, $p = 0.68$).

(**H**) $LH^{VGLUT2}$ activation in fasted mice decreases hunger. *Upper panel*, one-way repeated-measures ANOVA revealed a significant effect of photostimulation in $LH^{VGLUT2}$:ChR2 mice ($n = 5$; $F(2.08, 8.31) = 7.06$, $p = 0.016$; Dunnett's post-test: no stim vs. 2 Hz,$^{*}p = 0.042$; no stim vs. 5 Hz,$^{*}p = 0.016$; no stim vs. 10 Hz,$^{*}p = 0.016$; no stim vs. 20 Hz, $^{*}p = 0.015$) on fasted-associated lever responding. No significant effects were observed in YFP controls ($n = 6$; paired t test: $t(5) = 0.58$, $p = 0.59$). *Lower panel*, photostimulation significantly decreased response rate in $LH^{VGLUT2}$:ChR2 ($F(2.07, 8.28) = 10.60$, $p = 0.005$; Dunnett's post-test: no stim vs. 20 Hz, $^{*}p = 0.013$) but not $LH^{VGLUT2}$:YFP mice ($t(5) = 0.92$, $p = 0.40$).

(**I**) $LH^{VGLUT2}$ inhibition in sated mice does not induce hunger. *Upper panel*, two-way mixed-model ANOVA found no significant effects of $LH^{VGLUT2}$ inhibition on fasted-associated lever responding ($n = 5$ $LH^{VGLUT2}$:ChR2 and $n = 6$ $LH^{VGLUT2}$:YFP; group × treatment interaction: $F(1, 9) = 0.0035$, $p = 0.95$) or response rate (*lower panel*, $F(1, 9) = 1.20$, $p = 0.30$).

See also Figure S1.

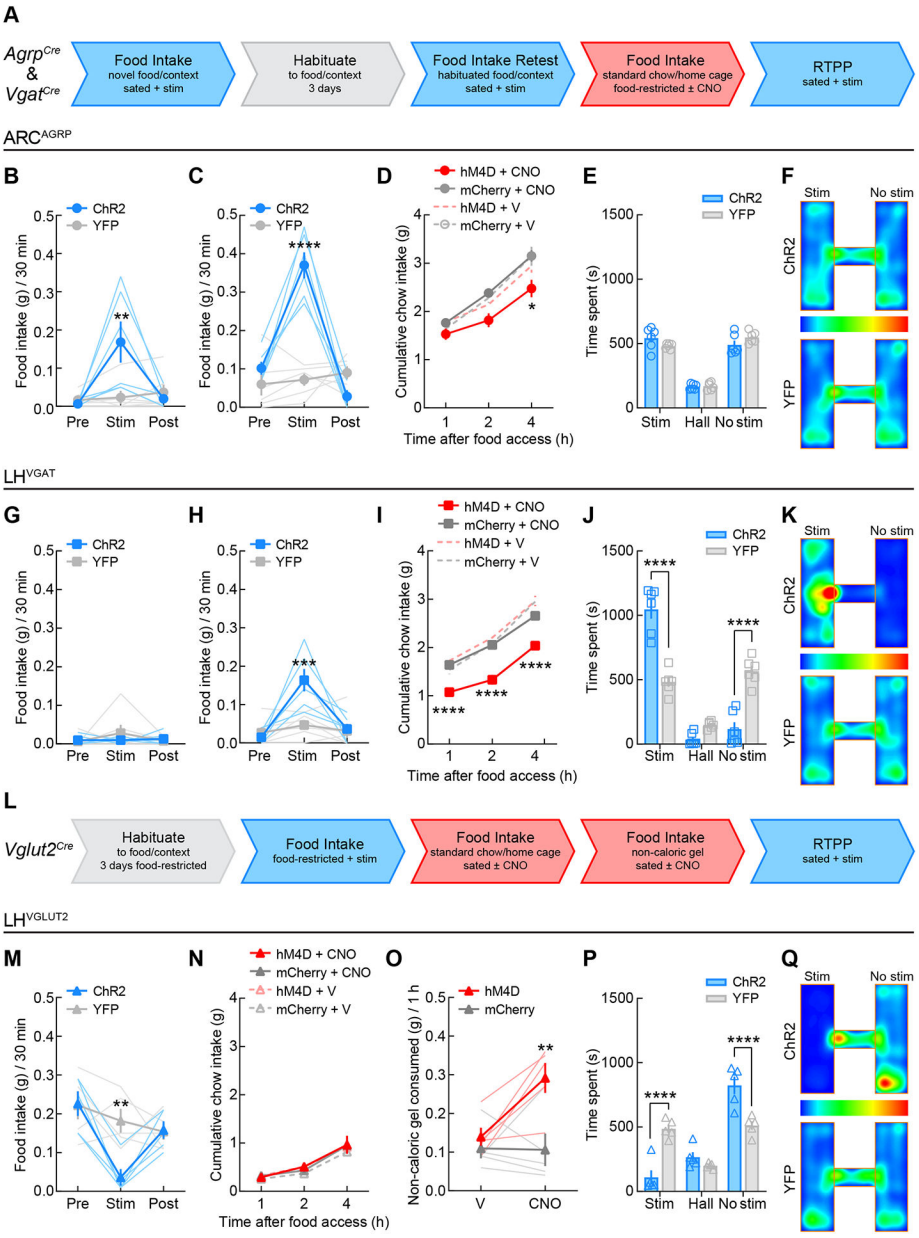


**Figure 3. Hypothalamic control of food intake and reward-related behavior.**

(**A**) Flowchart for testing *Agrp*$^{Cre}$ and *Vgat*$^{Cre}$ mice in assays of food intake and reward. Blue arrow segments indicate tests with optogenetic activation of neurons and red arrow segments indicate tests with chemogenetic inhibition of neurons.

(**B**) ARC$^{AGRP}$ activation in sated mice triggered consumption of novel food pellets in a novel context (two-way mixed-model ANOVA group × epoch interaction: $F(2, 20) = 8.32$, $p = 0.0023$; Bonferroni's post-test: $^{**}p = 0.001$) as well as (**C**) food pellet consumption following habituation ($F(2, 20) = 42.81$, $p < 0.0001$; Bonferroni's post-test: $^{****}p < 0.0001$). $n = 6$ mice per group.

(**D**) ARC$^{AGRP}$ inhibition in food-restricted mice decreased standard chow intake by 4 h post-food access (three-way mixed-model ANOVA revealed a significant main effect of time

($F$(2,18) = 193.9, $p < 0.0001$), with significant interactions of time × group ($F$(2, 18) = 5.07, $p = 0.18$) and treatment × group ($F$(1, 9) = 8.73, $p = 0.16$). Tukey's post-test revealed between-group differences in food intake during CNO treatment at 4 h post-food access, *$p = 0.015$). $n = 6$ $ARC^{AGRP}$:hM4D and $n = 5$ $ARC^{AGRP}$:YFP.

(**E**) $ARC^{AGRP}$ activation did not evoke reward- or aversive-like effects in the real-time place preference test ($n = 6$ mice per group; two-way mixed-model ANOVA group × chamber interaction: $F$(2, 20) = 2.54, $p = 0.10$).

(**F**) Group average location RTPP heat maps for $ARC^{AGRP}$:ChR2 ($n = 6$) and $ARC^{AGRP}$:YFP ($n = 6$) mice. Scale is percentage of time spent in location.

(**G**) $LH^{VGAT}$ activation in sated mice did not evoke food pellet intake under novel food and context conditions ($F$(2, 20) = 0.85, $p = 0.44$) and (**H**) only triggered intake post-habituation ($F$(2, 20) = 9.74, $p = 0.001$; Bonferroni's post-test: ***$p = 0.0001$). $n = 6$ mice per group.

(**I**) $LH^{VGAT}$ inhibition in food-restricted mice decreased standard chow intake throughout the 4 h feeding test (three-way mixed-model ANOVA revealed significant main effects of time ($F$(2,20) = 391.5, $p < 0.0001$), treatment ($F$(1, 10) = 64.00, $p < 0.0001$), and group ($F$(1, 10) = 15.59, $p = 0.0027$), with significant interactions of time × treatment ($F$(2, 20) = 19.01, $p < 0.0001$) and treatment × group ($F$(1, 10) = 45.02, $p < 0.0001$). Tukey's post-test revealed between-group differences in chow intake during CNO treatment at 1-, 2-, and 4-h post-food access (****$p < 0.0001$). $n = 6$ mice per group.

(**J**) $LH^{VGAT}$ activation triggered significant reward-like effects in the real-time place preference test ($n = 6$ mice per group; two-way mixed-model ANOVA group × chamber interaction: $F$(2, 20) = 45.13, $p < 0.0001$). Bonferroni's post-test revealed between-group differences in time spent in the stimulation-paired and -unpaired chambers (****$p < 0.0001$) but no differences in the time spent in the hallway compartment ($p = 0.25$).

(**K**) Group average location RTPP heat maps for $LH^{VGAT}$:ChR2 ($n = 6$) and $LH^{VGAT}$:YFP ($n = 6$) mice. Scale is percentage of time spent in location.

(**L**) Flowchart for testing $Vglut2^{Cre}$ mice. Blue arrow segments indicate tests with optogenetic activation of neurons and red arrow segments indicate tests with chemogenetic inhibition of neurons.

(**M**) $LH^{VGLUT2}$ activation in food-restricted mice significantly decreased standard chow intake ($F$(2, 16) = 5.88, $p = 0.012$; Bonferroni's post-test: **$p = 0.0035$). $n = 5$ $LH^{VGLUT2}$:ChR2 and $n = 6$ $LH^{VGLUT2}$:YFP.

(**N**) $LH^{VGLUT2}$ inhibition in sated mice did not change standard chow intake over 4 h (three-way mixed model ANOVA only revealed a significant main effect of time: $F$(2, 16) = 160.5, $p < 0.0001$) but (**O**) did increase intake of a novel non-caloric gel ($F$(1, 8) = 5.98, $p = 0.04$; Bonferroni's post-test: **$p = 0.0025$). $n = 5$ $LH^{VGLUT2}$:ChR2 and $n = 6$ $LH^{VGLUT2}$:YFP.

(**P**) $LH^{VGLUT2}$ activation triggered significant aversive-like effects in the real-time place preference test ($n = 5$ $LH^{VGLUT2}$:ChR2 and $n = 6$ $LH^{VGLUT2}$:YFP; two-way mixed-model ANOVA group × chamber interaction: $F$(2, 16) = 21.93, $p < 0.0001$). Bonferroni's post-test revealed between-group differences in time spent in the stimulation-paired and -unpaired chambers (****$p < 0.0001$) but no differences in the time spent in the hallway compartment ($p = 0.86$).

(**Q**) Group average location RTPP heat maps for $LH^{VGLUT2}$:ChR2 ($n = 5$) and $LH^{VGLUT2}$:YFP ($n = 6$) mice. Scale is percentage of time spent in location.

See also Figures S2–S4.

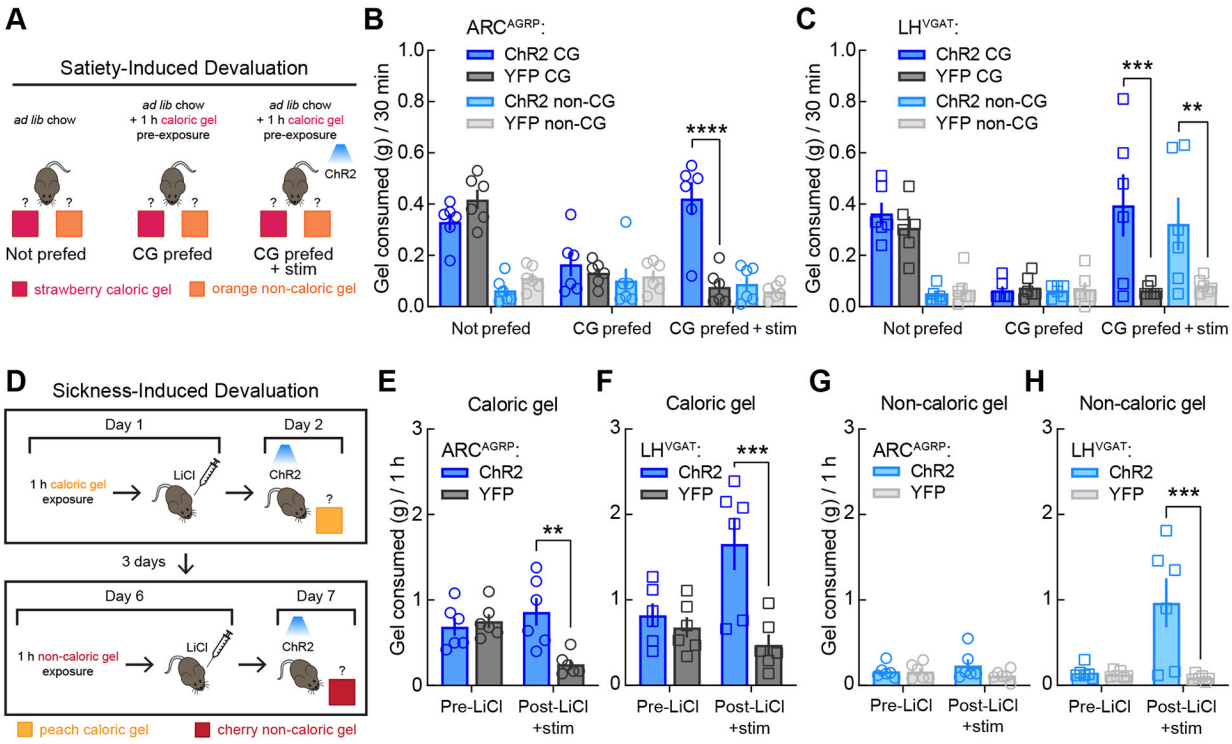


**Figure 4. Hypothalamic circuits for feeding are distinguished by calorie-specific versus indiscriminate food intake.**

(**A**) Schematic representation of satiety-induced devaluation. In test 1 (Not prefed), mice were housed with *ad libitum* chow and had 30-min simultaneous access to the caloric and non-caloric gels. In test 2 (CG prefed), mice had 1 h of access to caloric gel in the home cage prior to the 30-min choice session. Test 3 (CG prefed + stim) was the same as test 2 except that photostimulation was delivered during the 30-min choice session. $n = 6$ mice per group for all tests.

(**B**) $ARC^{AGRP}$ activation triggered calorie-specific gel intake following satiety-induced devaluation in the two-gel choice assay. A three-way mixed-model ANOVA revealed a significant test × calorie × group interaction, $F(2, 20) = 7.92$, $p = 0.0029$) and that among the two-factor interactions, the test × group interaction ($p = 0.0004$) accounted for the most variation. Thus, follow-up two-way (test × group) mixed-model ANOVAs within each gel revealed a significant test × group interaction for caloric gel ($F(2, 20) = 13.47$, $p = 0.0002$) but not non-caloric gel ($F(2, 20) = 1.13$, $p = 0.34$). Bonferroni's post-tests revealed that all mice displayed a significant decrease in caloric gel intake following 1 h caloric gel pre-exposure (CG prefed) as compared to normal *ad libitum* fed conditions (Not prefed, $p = 0.0001$) and that photostimulation increased caloric gel intake following devaluation in $ARC^{AGRP}$:ChR2 as compared to $ARC^{AGRP}$:YFP control mice (CG prefed + stim, ****$p < 0.0001$).

(**C**) $LH^{VGAT}$ activation triggered indiscriminate gel intake following satiety-induced devaluation in the two-gel choice assay. A three-way mixed-model ANOVA revealed no significant test × calorie × group interaction ($p = 0.63$) but that among the two-factor interactions, the test × group interaction ($p = 0.004$) accounted for the most variation. Thus, follow-up two-way (test × group) mixed-model ANOVAs within each gel revealed

significant test × group interactions for both caloric gel ($F(2, 20) = 4.95$, $p = 0.018$) and non-caloric gel ($F(2, 20) = 6.39$, $p = 0.0072$). Bonferroni's post-tests revealed that all mice displayed a significant decrease in caloric ($p = 0.0005$) but not non-caloric ($p > 0.99$) gel intake following 1 h caloric gel pre-exposure, but that photostimulation increased both caloric (***$p = 0.0008$) and non-caloric (**$p = 0.0019$) gel intake following devaluation in $LH^{VGAT}$:ChR2 as compared to $LH^{VGAT}$:YFP control mice.

(**D**) Schematic representation of sickness-induced devaluation. Mice were given access to caloric gel for 1 h followed by i.p. injection with LiCl. The following day, mice were exposed to the caloric gel during optogenetic stimulation and caloric gel consumption was measured. Three days later, LiCl-induced devaluation was repeated with a non-caloric gel. $n = 6$ mice per group for all tests.

(**E**) $ARC^{AGRP}$ activation triggered calorie-specific gel intake following LiCl-induced devaluation in single-gel test sessions ($F(1, 10) = 7.47$, $p = 0.021$; Bonferroni's post-test **$p = 0.0014$).

(**F**) $LH^{VGAT}$ activation evoked indiscriminate gel intake following LiCl-induced devaluation in single-gel test sessions (caloric gel: $F(1, 10) = 11.78$, $p = 0.0064$; Bonferroni's post-test: ***$p = 0.0005$).

(**G**) $ARC^{AGRP}$ activation did not affect non-caloric gel intake ($F(1, 10) = 2.18$, $p = 0.17$).

(**H**) $LH^{VGAT}$ activation evoked indiscriminate non-caloric gel intake following LiCl-induced devaluation in single-gel test sessions: $F(1, 10) = 9.13$, $p = 0.013$; Bonferroni's post-test: ***$p = 0.0007$).

## KEY RESOURCES TABLE

| REAGENT or RESOURCE | SOURCE | IDENTIFIER |
|---|---|---|
| **Antibodies** | | |
| chicken polyclonal anti-GFP | Aves Labs | Cat#GFP-1020; RRID:AB_10000240 |
| rabbit polyclonal anti-DsRed | Takara Bio, Inc. | Cat#632496; RRID:AB_10013483 |
| goat polyclonal anti-chicken Alexa Fluor 488 | Thermo Fisher Scientific | Cat#A11039; RRID:AB_2534096 |
| goat polyclonal anti-rabbit Alexa Fluor 647 | Thermo Fisher Scientific | Cat#A21245; RRID:AB_2535813 |
| **Bacterial and virus strains** | | |
| rAAV2/9-EF1α-double floxed-hChR2(H134R)-EYFP-WPRE-HGHpA | Karl Deisseroth, Stanford University | Addgene 20298-AAV9; RRID:Addgene_20298 |
| rAAV2/9-hSyn-DIO-hM4D(Gi)-mCherry | [25] | Addgene 44362-AAV9; RRID:Addgene_44362 |
| rAAV2/9-EF1α-DIO-EYFP | Karl Deisseroth, Stanford University | Addgene 27056-AAV9; RRID:Addgene_27056 |
| rAAV2/9-hSyn-DIO-mCherry | Bryan Roth, University of North Carolina | Addgene 50459-AAV9; RRID:Addgene_50459 |
| **Chemicals, peptides, and recombinant proteins** | | |
| rimonabant | Cayman Chemical | Cat#9000484 |
| bupropion | Cayman Chemical | Cat#10488 |
| lorcaserin | Cayman Chemical | Cat#15521 |
| liraglutide | Cayman Chemical | Cat#24727 |
| phentermine | Cayman Chemical | Cat#14207 |
| naltrexone hydrochloride | Millipore Sigma | Cat#N3136 |
| ghrelin | Anaspec | Cat#AS24159 |
| clozapine *N*-oxide (CNO) | Tocris Bioscience | Cat#4936 |
| lithium chloride (LiCl) | Teknova, Inc. | Cat#L0600 |
| **Experimental models: Organisms/strains** | | |
| Mouse: *Agrp*$^{tm1(cre)Lowl}$(*Agrp*$^{Cre}$) | The Jackson Laboratory | RRID:IMSR_JAX:012899 |
| Mouse: *Slc32a1*$^{tm2(cre)Lowl}$ (*Vgat*$^{Cre}$) | The Jackson Laboratory | RRID:IMSR_JAX:028862 |
| Mouse: *Slc17a6*$^{tm2(cre)Lowl}$ (*Vglut2*$^{Cre}$) | The Jackson Laboratory | RRID:IMSR_JAX:028863 |
| **Software and algorithms** | | |
| GraphicState v4 | Coulbourn Instruments | Cat#GS4.0; https://www.coulbourn.com/category_s/363.htm |
| Neuroscience Studio v5.1 | Doric Lenses, Inc. | RRID:SCR_018569; https://neuro.doriclenses.com/products/doric-neuroscience-studio |
| ANY-maze behavioral tracking software v5 | Stoelting Co. | RRID:SCR_014289; https://www.anymaze.co.uk/index.htm |
| Prism 8 | GraphPad | RRID:SCR_002798; https://www.graphpad.com/ |
| **Other** | | |
| PicoLab Rodent Diet 20 (5053) – 2.5 g Tablet | LabDiet | Cat#1815928 |
| PicoLab Rodent Diet 20 (5053) Pellet – 20 mg Pellet | LabDiet | Cat#1815928–372 |

| REAGENT or RESOURCE | SOURCE | IDENTIFIER |
|---|---|---|
| Sucrose Reward Pellet 5TUT – 20 mg Pellet | LabDiet | Cat#1811555 |
| Armour brand lard | Conagra Brands | N/A |
| sugar cubes | Domino Sugar | N/A |
| Reese's brand peanut butter chips | The Hershey Company | N/A |
| Snack Pack brand sugar-free orange flavored gelatin | Conagra Brands | N/A |
| Snack Pack brand strawberry flavored gelatin | Conagra Brands | N/A |
| Jello brand sugar-free lemon flavored gelatin | Kraft Heinz Company | N/A |
| Jello brand peach flavored gelatin | Kraft Heinz Company | N/A |
| Jello brand sugar-free cherry flavored gelatin | Kraft Heinz Company | N/A |